Appl. Phys. B (2014) 114:213–230
DOI 10.1007/s00340-013-5703-z

Applied Physics B
Lasers and Optics

The electric quadrupole moment of molecular hydrogen ions and their potential for a molecular ion clock

D. Bakalov · S. Schiller

Received: 6 July 2013 / Accepted: 16 October 2013 / Published online: 28 December 2013

Abstract The systematic shifts of the transition frequencies in the molecular hydrogen ions are of relevance to ultra-high-resolution radio-frequency, microwave and optical spectroscopy of these systems, performed in ion traps. We develop the ab initio description of the interaction of the electric quadrupole moment of this class of molecules with the static electric field gradients present in ion traps. In good approximation, it is described in terms of an effective perturbation Hamiltonian. An approximate treatment is then performed in the Born–Oppenheimer approximation. We give an expression of the electric quadrupole coupling parameter valid for all hydrogen molecular ion species and evaluate it for a large number of states of H_2^+, HD^+, and D_2^+. The systematic shifts can be evaluated as simple expectation values of the perturbation Hamiltonian. Results on radio-frequency, one-photon electric dipole (E1), and two-photon E1 transitions between hyperfine states in HD^+ are reported. For two-photon E1 transitions between rotationless states, the shifts vanish. For a large subset of rovibrational one-photon transitions, the absolute values of the quadrupole shifts range from 0.3 to 10 Hz for an electric field gradient of 10^8 V/m^2. We point out an experimental procedure for determining the quadrupole shift which will allow reducing its contribution to the uncertainty of unperturbed rovibrational transition frequencies to the 1×10^{-15} fractional level and, for selected transitions, even below it. The combined contributions of black-body radiation, Zeeman, Stark and quadrupole effects are considered for a large set of transitions, and it is estimated that the total transition frequency uncertainty of selected transitions can be reduced below the 1×10^{-15} level.

D. Bakalov
Institute for Nuclear Research and Nuclear Energy, Tsarigradsko chaussée 72, 1784 Sofia, Bulgaria

S. Schiller (✉)
Institut für Experimentalphysik, Heinrich-Heine-Universität Düsseldorf, 40225 Düsseldorf, Germany
e-mail: step.schiller@uni-duesseldorf.de

1 Introduction

One of the fascinating aspects of the ion trap invented by W. Paul and its later variants is the suitability for trapping a wide variety of particles. While atomic ions are the most frequently studied particle types, today, cold molecular ions are being studied in an increasing number of laboratories world-wide. The molecular ion most intensely studied so far from a spectroscopic point of view is the molecular hydrogen ion HD^+, for which significant progress has been made in the last decade, both on the experimental [1, 2] and on the ab-initio theory front (see Ref. [3] and references therein). Combined studies of HD^+ and of the isotopologue molecules (H_2^+ [4], HT^+ [5], D_2^+, etc.) may in the near future lead to the determination of several fundamental physical constants, such as the ratios of proton, deuteron, and triton mass relative to the electron mass, and the Rydberg energy [1, 6–8] with potentially competitive accuracy and with a different experimental approach than in atomic laser spectroscopy and Penning trap spectroscopy. A first step in this direction has been performed with two laser-spectroscopic measurements on HD^+ [1, 2], from which the ratio of the electron mass to the reduced nuclear mass can be inferred with a fractional experimental uncertainty of approximately 4 and 2 parts in 10^9, respectively.

Moreover, the molecular hydrogen ions may be suited to investigate the question whether the mentioned dimensionless fundamental constants are independent of time [7] and of location in space, a postulate made by the principle of local position invariance of General Relativity.

These possibilities are only feasible if the experimental uncertainty in the measurement of transition frequencies can be reduced to a level necessary for the particular application. For example, in order to make competitive determinations of the fundamental constants, (currently) uncertainties of 1×10^{-10} or less are desirable, while for the investigation of their time-independence, 1×10^{-16} or less is desirable. A series of systematic effects needs to be carefully taken into account, including the effects of the external electric and magnetic fields in the volume occupied by the molecular ions. The Zeeman shift of the transition frequency induced by the weak magnetic fields usually present in experiments was thoroughly investigated in [9–11]. Various aspects of the Stark effect of the HD^+ molecule have been studied in [12, 13], and recently in [14, 15].

In the present paper, we determine theoretically the energy shifts caused by the interaction of the permanent electric quadrupole moment of the molecular ion with the inhomogeneities of the electric field of the ion trap. For atomic ions used in optical clocks, this is a well-known systematic effect, but for molecular ions, this effect has not been treated before for any molecule, to the best of our knowledge.

Concerning related work, we mention that the electric quadrupole transitions of the molecular hydrogen ions have been of some theoretical interest. The transition matrix elements for H_2^+ have first been treated by Bates and Poots [16] and later more extensively in Refs. [17–19]; the value of the permanent quadrupole moment in the vibrational ground state $v = 0$ is reported in Refs. [16, 17, 20–21]. To our knowledge, there is only a single calculation concerning HD^+, namely of its permanent quadrupole moment in the level $v = 0$, in Ref. [22]. Recently, the quadrupole transition moments for D_2^+ have been reported [23].

After developing the general theory in Sect. 2, as in a previous work [15], the numerical calculations are performed in the Born–Oppenheimer approach, introduced in Sect. 3, which provides rovibrational energy levels and matrix elements with fractional error of approximately 10^{-3}, but is entirely sufficient for the evaluation of the electric quadrupole effect in ion traps. This will be justified *a posteriori* by the small size of the calculated corrections. The detailed study of a large number of transitions in HD^+ is given in Sect. 4. The discussion (Sect. 5) shows that Zeeman, electric quadrupole, and Stark shifts can be controlled to a sufficient level even in spectroscopy aiming for high accuracy.

2 Electric quadrupole shift in three-particle bound systems

In this section, we derive the general expressions for the quadrupole interaction effect in a three-body bound system.

We use the Jacobi coordinate vectors of the three-body system, $\mathbf{R}_C$, $\mathbf{R}$ and $\mathbf{r}$, which are related to the individual particle position vectors $\mathbf{R}_k$, $k = 1, 2, 3$ by means of

$$\begin{aligned}
&\mathbf{R}_C = \sum_{k=1}^{3} \frac{m_k}{m_t} \mathbf{R}_k, \\
&\mathbf{R} = \mathbf{R}_2 - \mathbf{R}_1, \\
&\mathbf{r} = \mathbf{R}_3 - \frac{m_1}{m_{12}} \mathbf{R}_1 - \frac{m_2}{m_{12}} \mathbf{R}_2, \\
&m_{kk'} = m_k + m_{k'}, \\
&m_{k,k'} = \frac{m_k m_{k'}}{m_{kk'}}, \\
&m_t = \sum_k m_k
\end{aligned} \tag{1}$$

where m_k are the masses of the particles. In the HD^+ ion, $k = 1, 2, 3$ labels the deuteron, the proton, and the electron, respectively. Note that $\mathbf{r}$ is defined as the radius vector of the electron reckoned from the center of mass of the two nuclei. In terms of the Jacobi vectors, the non-relativistic Hamiltonian H_{NR} splits into the sum of the free Hamiltonian H_C of the system "as a whole" and the Hamiltonian H of the internal degrees of freedom:

$$H_{NR} = H_C + H, H_C = \frac{\mathbf{P}_C^2}{2m_t}, \tag{2}$$

$$H = \frac{\mathbf{P}^2}{2m_{1,2}} + \frac{\mathbf{p}^2}{2m_{3,12}} + V(\mathbf{R}, \mathbf{r}), \tag{3}$$

$$V(\mathbf{R}, \mathbf{r}) = \sum_{k<k'} \frac{Z_k Z_{k'} e^2}{|\mathbf{R}_k - \mathbf{R}_{k'}|}, \tag{4}$$

where $\mathbf{P}_C$, $\mathbf{P}$ and $\mathbf{p}$ are the momenta conjugate to $\mathbf{R}_C$, $\mathbf{R}$ and $\mathbf{r}$, respectively, and Z_k are the particle charges in units of e.

In an external electric potential U, the non-relativistic Hamiltonian H_{NR} acquires an additional term: $H_{\mathrm{NR,ext}} = H_{\mathrm{NR}} + \Delta H$ with

$$\Delta H = \sum_{k=1}^{3} e Z_k U(\mathbf{R}_k) \tag{5}$$

being the electrostatic energy of the particles. For external fields that vary slowly in space and time, ΔH is approximated with the truncated multipole expansion

$$\begin{aligned}
&\Delta H = \Delta H_0 + \Delta H_d + \Delta H_Q, \\
&\Delta H_0 = (e \sum_k Z_k) U(\mathbf{R}_C), \\
&\Delta H_d = -\mathbf{d}_C \cdot \mathbf{E}(\mathbf{R}_C), \\
&\Delta H_Q = -\frac{1}{3} \Theta_C \cdot Q(\mathbf{R}_C),
\end{aligned} \tag{6}$$

where $\mathbf{d}_C$ is the electric dipole moment of the system with respect to $\mathbf{R}_C$, $\mathbf{d}_C = \sum_k e Z_k \mathbf{r}_k$, $\mathbf{r}_k = \mathbf{R}_k - \mathbf{R}_C$, Θ_C is the

irreducible tensor of rank 2 of the quadrupole moment with Cartesian components

$$(\Theta_C)_{ij} = (3/2)\sum_k eZ_k(r_{ki}r_{kj} - \delta_{ij}\mathbf{r}_k^2/3), \tag{7}$$

$$\mathbf{E}(\mathbf{R}_C) = -\nabla U(\mathbf{x})|_{\mathbf{x}=\mathbf{R}_C} \tag{8}$$

is the external electric field at the center point, and

$$Q(\mathbf{R}_C)_{ij} = -(\partial^2/\partial x_i \partial x_j)U(\mathbf{x})|_{\mathbf{x}=\mathbf{R}_C}. \tag{9}$$

ΔH_0, together with H_C, are dropped because of being related to the degrees of freedom of the 3-body system "as a whole". Different aspects of the second-order perturbation contribution of the dipole term have been evaluated in [12, 14, 15]. In what follows, we focus our attention on the contribution of the quadrupole interaction term ΔH_Q in first order of perturbation theory.

The Cartesian components $(\Theta_C)_{ij}$ in terms of the Cartesian components of the vectors $\mathbf{R}$ and $\mathbf{r}$ (in the center-of-mass frame $\mathbf{R}_C = 0$) are

$$(\Theta_C)_{ij} = \frac{3}{2}e\left(a_0\left(R_iR_j - \frac{\delta_{ij}}{3}\mathbf{R}^2\right) + a_1\left(\frac{R_ir_j + r_iR_j}{2} - \frac{\delta_{ij}}{3}\mathbf{R}\cdot\mathbf{r}\right) - a_2\left(r_ir_j - \frac{\delta_{ij}}{3}\mathbf{r}^2\right)\right), \tag{10}$$

$$a_0 = (m_1^2 + m_2^2)/m_{12}^2,\ a_1 = 2(m_2 - m_1)m_3/(m_{12}m_t),$$
$$a_2 = (m_{12}^2 - 2m_3^2)/m_t^2. \tag{11}$$

Note the factor 3/2 in the definition of Θ_C that is not present in the analogous expressions in Refs. [16, 22]. In evaluating the matrix elements of Θ_C in the angular momentum representation, similar to Refs. [24, 25] we use the expansion of the non-relativistic three-body wave function of the bound state with the orbital momentum quantum number L, the projection of $\mathbf{L}$ on the space-fixed z-axis equal to M, the vibrational quantum number v and the parity λ in the basis of the symmetrized Wigner functions $\mathcal{D}^{\lambda L}_{Mm}$,

$$\psi^{\lambda vLM}(\mathbf{R},\mathbf{r}) = \langle \mathbf{R},\mathbf{r}|\lambda vLM\rangle = \sum_{m=0}^{L} u_m^{\lambda vL}(R,r,\gamma)\mathcal{D}^{\lambda L}_{Mm}(\Phi,\theta,\varphi), \tag{12}$$

where γ is the angle between the vectors $\mathbf{R}$ and $\mathbf{r}$: $\cos\gamma = \mathbf{R}\cdot\mathbf{r}/(Rr)$, while Φ, θ and φ are the Euler angles of the rotation that transforms the space-fixed into the body-fixed reference frame with z-axis along $\mathbf{R}$ and $\mathbf{r}$ in the xOz plane.

The amplitudes $u_m^{\lambda vL}(R, r, \gamma)$ are normalized by the condition $\int \mathrm{d}RR^2 \int \mathrm{d}rr^2 \int \mathrm{d}\gamma \sin\gamma \sum_m (u_m^{\lambda vL}(R,r,\gamma))^2 = 1$.

The normalized symmetrized Wigner functions $\mathcal{D}^{\lambda L}_{Mm}(\Phi,\theta,\varphi)$ are linear combinations with definite parity of the complex conjugated standard Wigner functions:

$$\mathcal{D}^{\lambda L}_{Mm}(\Phi,\theta,\varphi) = \sqrt{\frac{2L+1}{16\pi^2(1+\delta_{0m})}}\big((-1)^m D^{L*}_{Mm}(\Phi,\theta,\varphi) + \lambda(-1)^L D^{L*}_{M-m}(\Phi,\theta,\varphi)\big). \tag{13}$$

Next, the cyclic components of the quadrupole moment $\tilde{\Theta}_C$ (labeled with the tilde to distinguish from the Cartesian components) are put in the form of a sum of terms with factorized dependence on the sets of angular and radial variables:

$$\tilde{\Theta}_C = e\Big(a_0R^2X^0 + a_1Rr\big(d^1_{00}(\gamma)X^0 - \frac{\sqrt{3}}{2}d^1_{10}(\gamma)X^1\big) - a_2r^2\big(d^2_{00}(\gamma)X^0 + d^2_{10}(\gamma)X^1 + d^2_{20}(\gamma)X^2\big)\Big), \tag{14}$$

where $d^L_{mM}(\gamma)$ are the "small" Wigner d-matrices given in [26]. The $(X^i)_0$, $i = 0, 1, 2$ are the 0th cyclic components of irreducible tensor operators X^i of rank 2 acting on the angular variables:

$$(X^0)_0 = \frac{3}{2}\cos^2\theta - \frac{1}{2},\quad (X^1)_0 = \sqrt{6}\sin\theta\cos\theta\cos\varphi,$$
$$(X^2)_0 = \sqrt{\frac{3}{2}}\sin^2\theta\cos 2\varphi. \tag{15}$$

The reduced matrix elements of X^i in the angular basis of Eq. (13) have the form:

$$\begin{aligned}
\langle\lambda'm'L'||X^0||\lambda mL\rangle &= N(C^{L'm'}_{Lm,20} + \sigma C^{L'm'}_{L-m,20}),\\
\langle\lambda'm'L'||X^1||\lambda mL\rangle &= N(C^{L'm'}_{Lm,2-1} - C^{L'm'}_{Lm,21}\\
&\quad + \sigma(C^{L'm'}_{L-m,2-1} - C^{L'm'}_{L-m,21})),\\
\langle\lambda'm'L'||X^2||\lambda mL\rangle &= N(C^{L'm'}_{Lm,2-2} + C^{L'm'}_{Lm,22}\\
&\quad + \sigma(C^{L'm'}_{L-m,2-2} + C^{L'm'}_{L-m,22})),
\end{aligned} \tag{16}$$

where $N = \delta_{\lambda\lambda'}\sqrt{(2L+1)/((1+\delta_{0m})(1+\delta_{0m'}))}$, $\sigma = \lambda(-1)^{m+L}$, and $C^{e\varepsilon}_{a\alpha,b\beta} \equiv \langle e\varepsilon|a\alpha, b\beta\rangle$ are the Clebsch–Gordan coefficients.

Thus, the matrix elements of ΔH_Q in the basis Eq. (12) become

$$\langle\lambda v'L'M'|\Delta H_Q|\lambda vLM\rangle = -\frac{1}{3}\left(\sum_{q=-2}^{2}\tilde{Q}^q(\mathbf{R}_C)C^{L'M'}_{LM,2q}\right) \times (2L'+1)^{-1/2}\langle\lambda v'L'||\tilde{\Theta}_C||\lambda vL\rangle, \tag{17}$$

$$\begin{aligned}
\langle\lambda v'L'||\tilde{\Theta}_C||\lambda vL\rangle &= e\sum_{m'm}\Big(\langle\lambda m'L'||X^0||\lambda mL\rangle\\
&\quad\times\Big(a_0I^{(00)m'm}_{\lambda,v'L',vL} + a_1I^{(01)m'm}_{\lambda,v'L',vL} - a_2I^{(02)m'm}_{\lambda,v'L',vL}\Big)\\
&\quad-\langle\lambda m'L'||X^1||\lambda mL\rangle\Big(\frac{\sqrt{3}}{2}a_1I^{(11)m'm}_{\lambda,v'L',vL} + a_2I^{(12)m'm}_{\lambda,v'L',vL}\Big)\\
&\quad-\langle\lambda m'L'||X^2||\lambda mL\rangle a_2I^{(22)m'm}_{\lambda,v'L',vL}
\end{aligned} \tag{18}$$

where $\tilde{Q}^q$ are the contravariant cyclic components of Q and $I^{(kn)m'm}_{\lambda,\nu'L',\nu L}$ denote the following integrals,

$$I^{(kn)m'm}_{\lambda,\nu'L',\nu L} = \int \mathrm{d}RR^2 \int \mathrm{d}rr^2 \int \mathrm{d}\gamma \sin(\gamma) u^{\lambda\nu'L'}_{m'} \times (R,r,\gamma) R^{2-n} r^n \mathrm{d}^n_{k0}(\gamma) u^{\lambda\nu L}_{m}(R,r,\gamma). \quad (19)$$

Equations (14–18), after the appropriate changes of variables in Eqs. (14) and (19) can be used with any alternative choice of the arguments of the radial amplitudes u in the expansion Eq. (12), e.g. the variables $|\mathbf{R}_k - \mathbf{R}_{k'}|, k<k'$ or their linear combinations [25], but need be reworked for alternative basis sets in the space of functions of the angular variables, such as the expansion in bi-harmonics of Refs. [6, 27].

The quadrupole term $\Delta H_Q = -(1/3)\Theta_C \cdot Q(\mathbf{R}_C)$ in the expansion Eq. (6) couples, in the general case, states with different values of the orbital momentum L and its projection M and shifts the energy levels of the three-body states by amounts that depend on M.

Previous studies of the effects of external magnetic fields [10, 11] had demonstrated the advantages of considering the various perturbations to the dominating Coulomb interactions due to relativistic effects, particle spin and external fields on the same footing. An efficient implementation of these calculations in first order of perturbation theory is the use of an "effective Hamiltonian" H_{eff}. We remind that the "effective spin Hamiltonian" of an atomic system is the projection of the spin interaction operator on the finite dimensional space of eigenstates of the non-relativistic Hamiltonian of the system with definite values of the orbital angular momentum and the remaining non-relativistic quantum numbers, in which couplings to different L are neglected.

We therefore include the effects of the quadrupole interaction ΔH_Q in the form of an additional term V^{Q} in the effective spin Hamiltonian $H^{\mathrm{hfs}}_{\mathrm{eff}}$, introduced in [28] (denoted by H_{eff} there) in the calculation of the hyperfine structure and completed to $H^{\mathrm{tot}}_{\mathrm{eff}} = H^{\mathrm{hfs}}_{\mathrm{eff}} + V^{\mathrm{mag}}$ by terms V^{mag} that describe the Zeeman shifts in [10, 11]. That is, we set

$$V^{\mathrm{Q}}(v,L) = E_{14}(v,L) Q(\mathbf{R}_C) \cdot (\mathbf{L} \otimes \mathbf{L})^{(2)},$$
$$H^{\mathrm{tot+Q}}_{\mathrm{eff}}(v,L) = H^{\mathrm{hfs}}_{\mathrm{eff}}(v,L) + V^{\mathrm{mag}}(v,L) + V^{\mathrm{Q}}(v,L), \quad (20)$$

where $(\mathbf{L}\otimes\mathbf{L})^{(2)}$ is the tensor square of the orbital momentum operator $\mathbf{L}$—the only irreducible tensor operator of rank 2 acting in the space of states with definite value of L. In Eq. (20), we have shown explicitly the dependence of the effective Hamiltonian and its various terms on the quantum numbers (v, L) of the non-relativistic state to which they refer. From the next section on, in order to simplify the notations we shall omit these quantum numbers while keeping in mind the dependence on them. The advantage of using the effective Hamiltonian is that the integrals of the 3-body wave functions of Eqs. (28) or (12) over R, r and γ are encoded in the single constant E_{14}, so that the electric quadrupole shift of each individual quantum state is calculated by standard angular momentum algebra.

The expression for E_{14} reads:

$$E_{14}(v,L) = -\frac{1}{3}\frac{\langle \lambda\nu L||\tilde{\Theta}_C||\lambda\nu L\rangle}{\langle L||(\mathbf{L}\otimes\mathbf{L})^{(2)}||L\rangle},$$
$$\langle L||(\mathbf{L}\otimes\mathbf{L})^{(2)}||L\rangle = \sqrt{\frac{\Gamma(2L+4)}{4!\Gamma(2L-1)}}. \quad (21)$$

3 Born–Oppenheimer approximation

The gradient of the electric field acting on an ion in a tightly confining quadrupole ion trap is of the order of 10^8 V/m^2 and in what follows it will be shown that this magnitude gives rise to energy level shifts not exceeding 100 Hz, significantly below the Zeeman shifts of most levels for the typical fields that are applied in ion traps [9–11]. This situation softens the requirements to the numerical and theoretical accuracy of the treatment and allows for using the Born–Oppenheimer wave functions instead of the highly accurate variational wave functions of Ref. [29].

The Born–Oppenheimer approximation assumes that instead of $\mathbf{R}_C$ the molecular ion's "motion as a whole" is associated with the nuclear center-of-mass position vector $\mathbf{R}_B = (m_1\mathbf{R}_1 + m_2\mathbf{R}_2)/m_{12}$ and its conjugate momentum $\mathbf{P}_B$. H_{NR} then takes the form

$$H_{\mathrm{NR}} = H_B + \Delta H_B + H,$$
$$H_B = \frac{\mathbf{P}_B^2}{2m_{12}},$$
$$\Delta H_B = \frac{2}{m_{12}}(\mathbf{P}_B \cdot \mathbf{p}), \quad (22)$$

where H is that part that depends only on the internal degrees of freedom. Separation of external and internal degrees of freedom occurs by neglecting the cross term ΔH_B. This neglect limits *a priori* the fractional in accuracy of the results to the magnitude of the omitted terms of order $O(4\ m_3/m_{12}) \sim 10^{-3}$. The inaccuracy due to the replacement of m_t in the denominator of H_C in Eq. (2) by m_{12} in H_B is smaller.

In order to further separate the degrees of freedom of the electron from the relative motion of the nuclei, we expand the wave function of the eigenstates of H in the basis of eigenfunctions of the electronic Hamiltonian:

$$\psi^{\lambda\nu LM}(\mathbf{R},\mathbf{r}) = \sum_c \psi^{(\mathrm{N})\lambda\nu LM}_c(\mathbf{R}) \psi^{(\mathrm{e})}_c(\mathbf{r};R)\ , \quad (23)$$

$$(H^{(\mathrm{e})} - E_c(R))\psi_c^{(\mathrm{e})}(\mathbf{r};R) = 0\ , \tag{24}$$

$$H = H^{(\mathrm{N})} + H^{(\mathrm{e})}, \quad H^{(\mathrm{N})} = \frac{1}{2m_{1,2}}\mathbf{P}^2 + \frac{e^2}{R},$$

$$H^{(\mathrm{e})} = \frac{1}{2m_{3,12}}\mathbf{p}^2 - \sum_{k=1,2}\frac{e^2}{|\mathbf{R}_3 - \mathbf{R}_k|}. \tag{25}$$

We solved Eq. (24) numerically using its separability in the prolate spheroidal coordinates

$$\xi = \frac{1}{R}(|\mathbf{R}_3 - \mathbf{R}_1| + |\mathbf{R}_3 - \mathbf{R}_2|),$$
$$\eta = \frac{1}{R}(|\mathbf{R}_3 - \mathbf{R}_1| - |\mathbf{R}_3 - \mathbf{R}_2|)\ , \tag{26}$$

Their definition ranges are $1 \le \xi < \infty$, $-1 < \eta < 1$. These coordinates are related to r and γ of Eq. (12) by means of

$$r = R\sqrt{\frac{m_1}{m_{12}}\left(\frac{\xi+\eta}{2}\right)^2 + \frac{m_2}{m_{12}}\left(\frac{\xi-\eta}{2}\right)^2 - \frac{m_1 m_2}{m_{12}^2}},$$
$$\cos\gamma = \frac{R}{2r}\left(\xi\eta + \frac{m_1 - m_2}{m_{12}}\right). \tag{27}$$

We reproduced the results for $E_k(R)$ of Ref. [30].

The calculations of the dipole polarizabilities of the lower rovibrational states of HD^+ in Ref. [15] have shown (by comparison with the high precision variational results of Ref. [31]) that a fractional error of 10^{-3} in the computation of the energy values and of the dipole moments may be reached by keeping only the first term $c = (1s\sigma)$ in the expansion Eq. (24) and by neglecting the diagonal correction term $\langle\psi_{1s\sigma}^{(\mathrm{e})}|\mathbf{P}^2|\psi_{1s\sigma}^{(\mathrm{e})}\rangle$. We therefore adopted this approximation in the evaluation of the quadrupole shift as well and took the wave functions of "normal" parity $\lambda = +1$ (the index λ is omitted in what follows) in the form:

$$\psi^{vLM}(\mathbf{R},\mathbf{r}) = R^{-1}\chi_{1s\sigma}^{vL}(R)\mathrm{Y}_{LM}(\Phi,\theta)\psi_{1s\sigma}^{(\mathrm{e})}(\xi,\eta;R)\ , \tag{28}$$

with normalization conditions

$$\frac{R^3}{8}\int\int \mathrm{d}\xi\mathrm{d}\eta(\xi^2-\eta^2)\psi_{1s\sigma}^{(\mathrm{e})}(\xi,\eta;R)^2 = 1\ , \tag{29}$$

$$\int_0^\infty \mathrm{d}R\chi_{1s\sigma}^{vL}(R)^2 = 1. \tag{30}$$

We calculated numerically the $\chi_{1s\sigma}^{vL}(R)$ as solutions of the radial Schrödinger equation.

One could then obtain E_{14} by using Eq. (21) and evaluating the integrals in Eq. (19) with the wave functions of Eq. (28). Instead, we re-expand ΔH of Eq. (6) around the "Born–Oppenheimer central point" $\mathbf{R}_B$ so that the quadrupole interaction term takes the form

$$\Delta H_Q = -(1/3)\Theta_B \cdot Q(\mathbf{R}_B). \tag{31}$$

The tensor Θ_B differs from Θ_C of Eq. (10) by terms of order $O(a_1) \sim 10^{-4}$ or smaller:

$$(\Theta_B)_{ij} = e\frac{3}{2}\left(a_0\left(R_iR_j - \frac{\delta_{ij}}{3}\mathbf{R}^2\right) - \left(r_ir_j - \frac{\delta_{ij}}{3}\mathbf{r}^2\right)\right). \tag{32}$$

and the error due to replacing Θ_C by Θ_B is within the adopted accuracy limits. Note that $a_0 = \frac{1}{2}$ for the homonuclear ions H_2^+, D_2^+, T_2^+ but differs for the heteronuclear ones.

Similar to Eq. (14), we expand the cyclic components $\tilde{\Theta}_B$ over the set of irreducible tensor operators X^i, but keep only the terms involving X^0 since the matrix elements of X^i, $i \ge 1$ vanish in the σ-term approximation with $m' = m = 0$, adopted in Eq. (28):

$$\tilde{\Theta}_B \approx e\big(a_0R^2 - r^2d_{00}^2(\gamma)\big)X^0. \tag{33}$$

In order to facilitate comparison with the results of earlier papers on the subject, instead of using the more general notations of Eq. (19), we put the reduced matrix elements of $\tilde{\Theta}_B$ in the form:

$$\langle\lambda v'L'||\tilde{\Theta}_B||\lambda vL\rangle \approx \langle\lambda 0L'||X^0||\lambda 0L\rangle\overline{M}_{v'L',vL},$$
$$\overline{M}_{v'L',vL} = e\int_0^\infty \mathrm{d}R\chi_{1s\sigma}^{v'L'}(R)M(R)\chi_{1s\sigma}^{vL}(R),$$
$$M(R) = R^2\left(\frac{1}{2} - \frac{m_1m_2}{m_{12}^2}\right) + F(R),$$
$$F(R) = R^2\left(\frac{1}{2} + \frac{R^3}{8}\int \mathrm{d}\xi\mathrm{d}\eta(\xi^2-\eta^2)\right.$$
$$\left.\times\frac{1}{8}(\xi^2+\eta^2-3-3\xi^2\eta^2)\left(\psi_{1s\sigma}^{(e)}(\xi,\eta;R)\right)^2\right). \tag{34}$$

We have made use of the symmetry of the wave function squared $\psi_{1s\sigma}^{(e)\,2}$ with respect to $\eta \to -\eta$, so that only terms with even powers of η contribute.

The function $M(R)$ may also be expressed as $M(R) = R^2(m_1^2 + m_2^2)/m_{12}^2 + \langle z^2\rangle + \langle x^2\rangle$ (the angular brackets refer to the averaging over the electronic coordinates with $\psi_{1s\sigma}^{(\mathrm{e})}$). Note that $F(R)$ is independent of the molecular species and $M(R)$ is the same for all homonuclear species: $M(R)|_{m_1=m_2} = R^2/4 + F(R)$. The function $F(R)$, which gives the correction to the asymptotic behavior of $M(R)$, was introduced in [17]. In Fig. 1 we plot it.

3.1 Comparison with previous work

The values of $M(R)$ for homonuclear ions, calculated with our numerical values of the function $F(R)$, agree with the

results of Refs. [16] (Table 1 therein), [21] (Table 2 therein) and [32]. Also, the values of the function $F(R)$ are essentially identical to those extracted from Ref. [17] in their Table II.

For H_2^+, our value $\overline{M}_{00,00} = 1.63775$ a.u. is in agreement with Ref. [20] (Table 1 therein) and the numerically less accurate, older value of Ref. [16] (Table 3 therein). Our values $\overline{M}_{0L,0L}, L = 0, \ldots 10$, agree within 0.001 atomic units with the more accurate values of Ref. [21] (Table 3 therein) computed with the adiabatic potential.

Concerning HD^+ the only previous calculation known to us is Ref. [22] (Table 1). There, the definition of the quadrupole moment is $\langle \frac{1}{2}(R^2 + r^2 - 3z^2) \rangle$, the same as for the homonuclear ions. Thus, the expression $M(R)|_{BD} = R^2 m_1 m_2 / m_{12}^2 + F(R)$ was used, which involves a different dependence on the nuclear masses as compared with our Eq. (34). Our definition of the quadrupole moment for HD^+ is $\langle (\Theta_B)_{zz} \rangle = \left\langle \left(\tilde{\Theta}_B\right)_0 \right\rangle = \langle \frac{1}{2}(2a_0 R^2 + r^2 - 3z^2) \rangle$. Accordingly, our value of $\overline{M}_{00,00} = 1.7409$ a.u. differs from $\overline{M}_{00,00}|_{BD} = 1.505729$ a.u. (table I in Ref. [22]). However, if we compute $M(R)|_{BD}$ with the functions $\chi^{00}_{1s\sigma}(R)$ calculated in the present work, we obtain a similar result, $\overline{M}'_{00,00} = 1.5042$ a.u., which clearly indicates that the discrepancy is due to the different analytical expressions used, not to different wave functions.

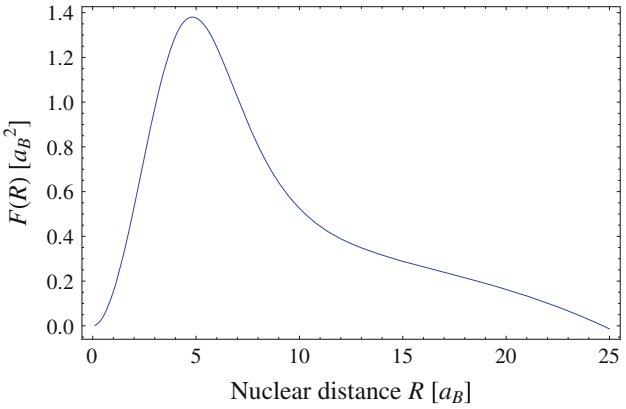

Fig. 1 Plot of the function $F(R)$ (in atomic units)

3.2 The quadrupole coupling coefficients in the effective Hamiltonian E_{14}

Equations (21, 34) lead to the following expression of the quadrupole coupling coefficients E_{14} of the effective Hamiltonian for the rovibrational state (v, L) in the adopted approximation:

$$E_{14} = e \frac{\sqrt{6}}{3(2L-1)(2L+3)} \overline{M}_{vL,vL}. \tag{35}$$

Tables 1, 2 and 3 list the values of E_{14} for 99 rovibrational states of HD^+, H_2^+ and D_2^+, respectively, calculated using Eq. (35). Note the slow increase of E_{14} with v and the stronger decrease with L. The entries with $L = 0$ are not of relevance in the following, but are given for completeness since they are proportional to the normalized quadrupole moment of the $L = 0$ states, $\overline{M}_{v0,v0} = -9E_{14}(v, 0)/\sqrt{6}$.

4 The quadrupole shift in HD^+

4.1 Generalities

We denote by $E^{vLnJ_z}(\mathbf{B}, Q)$ the energy of the hyperfine state $|vLnJ_z(\mathbf{B}, Q)\rangle$ of HD^+ in a magnetic field $\mathbf{B}$ and in an electric field gradient Q. Because of the spin interactions these states are not in general eigenstates of the operators $\mathbf{F}^2$, $\mathbf{S}^2$ and $\mathbf{J}^2$ and the quantum numbers F, S and J associated with them are not exact quantum numbers, but for

Table 1 Numerical values of the coefficients E_{14} of the effective Hamiltonian, Eq. (20), for some rovibrational states (v, L) of HD^+, with units MHz m^2/GV

L	$v = 0$	1	2	3	4	5	6	7	8
0	−0.3208(−3)	−0.3607(−3)	−0.4032(−3)	−0.4486(−3)	−0.4972(−3)	−0.5494(−3)	−0.6056(−3)	−0.6664(−3)	−0.7324(−3)
1	0.1928(−3)	0.2168(−3)	0.2423(−3)	0.2696(−3)	0.2988(−3)	0.3302(−3)	0.3640(−3)	0.4005(−3)	0.4402(−3)
2	0.4609(−4)	0.5180(−4)	0.5790(−4)	0.6441(−4)	0.7139(−4)	0.7888(−4)	0.8693(−4)	0.9565(−4)	0.1051(−3)
3	0.2163(−4)	0.2430(−4)	0.2716(−4)	0.3021(−4)	0.3348(−4)	0.3699(−4)	0.4077(−4)	0.4485(−4)	0.4930(−4)
4	0.1273(−4)	0.1430(−4)	0.1598(−4)	0.1777(−4)	0.1969(−4)	0.2176(−4)	0.2398(−4)	0.2638(−4)	0.2900(−4)
5	0.8454(−5)	0.9495(−5)	0.1061(−4)	0.1179(−4)	0.1307(−4)	0.1443(−4)	0.1591(−4)	0.1750(−4)	0.1924(−4)
6	0.6059(−5)	0.6803(−5)	0.7596(−5)	0.8446(−5)	0.9355(−5)	0.1033(−4)	0.1139(−4)	0.1253(−4)	0.1377(−4)
7	0.4580(−5)	0.5140(−5)	0.5738(−5)	0.6377(−5)	0.7062(−5)	0.7799(−5)	0.8595(−5)	0.9456(−5)	0.1040(−4)
8	0.3601(−5)	0.4040(−5)	0.4508(−5)	0.5009(−5)	0.5546(−5)	0.6124(−5)	0.6747(−5)	0.7424(−5)	0.8164(−5)
9	0.2920(−5)	0.3273(−5)	0.3651(−5)	0.4056(−5)	0.4490(−5)	0.4957(−5)	0.5461(−5)	0.6010(−5)	0.6609(−5)
10	0.2426(−5)	0.2718(−5)	0.3031(−5)	0.3365(−5)	0.3724(−5)	0.4111(−5)	0.4530(−5)	0.4985(−5)	0.5483(−5)

The notation $a(-b)$ stands for $a \times 10^{-b}$. In order to convert the values to atomic units ($e\, a_B^2$), multiply by 1476.87

weak fields may be considered as approximate quantum numbers. For given values of L and J_z, the number $N(L, J_z)$ of eigenstates $|vLnJ_z(\mathbf{B}, Q)\rangle$ is equal to the number of the combinations of quantum numbers (F, S, J) in the spin coupling scheme of Refs. [10, 11] allowed by angular momentum algebra. We therefore use the index $n = 1, 2, \ldots, N(L, J_z)$, which enumerates the possible combinations of (F, S, J), to label the spin content of $|vLnJ_z(\mathbf{B}, Q)\rangle$ and associate each value of n with the set of values of the approximate quantum numbers: $n \Leftrightarrow (F_n, S_n, J_n)$. Note that J is exact in the absence of external fields, and J_z is exact if the axial symmetry is conserved.

We consider in the following three levels of perturbation calculations, which are all restricted to a given level (v, L): (1) diagonalizing the whole effective Hamiltonian $H_{\rm eff}^{\rm tot+Q}$ between angular momentum basis states; (2) diagonalizing the matrix of the quadrupole interaction $V^{\rm Q}$ between eigenstates of the effective Hamiltonian $H_{\rm eff}^{\rm tot}$ that includes magnetic, but not the quadrupole interaction; (3) computing the expectation value of the quadrupole interaction. We then show that the latter approximation is sufficient.

4.2 Diagonalization of the effective Hamiltonian in a state (v, L)

The energies $E^{vLnJ_z}(\mathbf{B}, Q)$ are defined as eigenvalues of the matrix of the effective spin Hamiltonian $H_{\rm eff}^{\rm tot+Q}$ of Eq. (20) in the subspace of states with fixed values of v and L. This matrix has dimension $(2S_p + 1)(2S_d + 1)(2S_e + 1)(2L + 1)$ squared (S_p, S_d, S_e being the spins of the three particles), i.e. $12(2L + 1) \times 12(2L + 1)$. The matrix elements of the spin interaction operators (the first 9 terms of $H_{\rm eff}^{\rm tot+Q}$) were computed in [28] and those of the interactions with external magnetic field $V^{\rm mag}$ (next 4 terms) in [10, 11]. With account of Eqs. (34) and (35), the matrix elements of the projection $V^{\rm Q}$ of ΔH_Q on the subspace of a state with fixed values of v and L have the form:

$$\begin{aligned}\left\langle vLF'S'J'J'_z|V^{Q}|vLFSJJ_z\right\rangle &= E_{14}\delta_{S'S}\delta_{F'F}(-1)^{J'+S+L}\\ &\times\langle L||(\mathbf{L}\otimes\mathbf{L})^{(2)}||L\rangle\times\sqrt{2J+1}\begin{Bmatrix} L & 2 & L\\ J' & S & J\end{Bmatrix}\sum_q \tilde{Q}^q(\mathbf{R}_B)C^{J'J'_z}_{JJ_z,2q}.\end{aligned} \tag{36}$$

Note that they vanish for $L = 0$ levels.

4.3 Diagonalization of the electric quadrupole Hamiltonian in the space of Zeeman hyperfine states

Comparison of the values of E_{14} with the values of the coefficients $E_k, k = 10, \ldots, 13$ of the effective Hamiltonian for the Zeeman effect [10, 11] shows that, for the electric field gradients and magnetic fields of interest here, the quadrupole shift $\Delta E_{\rm Q}^{vLnJ_z} = E^{vLnJ_z}(\mathbf{B}, Q) - E^{vLnJ_z}(\mathbf{B}, 0)$ is, for the majority of levels, much smaller than the Zeeman shift $E^{vLnJ_z}(\mathbf{B}, 0) - E^{vLnJ_z}(0, 0)$. Even the hyperfine states least sensitive to magnetic fields, those with $J_z = 0$ (having only a quadratic Zeeman shift), exhibit at 1 G a typical shift of a few kHz or more, occasionally only tens of Hz, while the electric quadrupole shift, in a 10^8 V/m^2 gradient, is on the order of 100 Hz. Therefore, for sufficiently large magnetic fields the electric quadrupole shift can conveniently be evaluated as a perturbation to the Zeeman-shifted hyperfine energy levels by diagonalizing the matrix of $V^{\rm Q}$, Eq. (20), in the basis of the Zeeman-shifted hyperfine states $|vLnJ_z(\mathbf{B}, 0)\rangle$, calculated as eigenvectors of the spin and magnetic interaction part $H_{\rm eff}^{\rm tot+Q} = H_{\rm eff}^{\rm hfs} + V^{\rm mag}$ of the effective Hamiltonian of Eq. (20):

$$\begin{aligned}\left\langle vLn'J'_z(B,0)|V^{\rm Q}|vLnJ_z(B,0)\right\rangle &= E_{14}\langle L||(L\otimes L)^{(2)}||L\rangle\\ &\times\sum_q\tilde{Q}^q(\mathbf{R}_B)\sum_{FSJ'J}(-1)^{S+J'+L}\sqrt{2J+1}\\ &\times\begin{Bmatrix} L & 2 & L\\ J' & S & J\end{Bmatrix}C^{J'J'_z}_{JJ_z,2q}\beta^{vLn'J'_z}_{FSJ'}(\mathbf{B})\beta^{vLnJ_z}_{FSJ}(\mathbf{B}),\end{aligned} \tag{37}$$

where $\beta^{vLnJ_z}_{FSJ}(\mathbf{B})$ are the expansion coefficients of the hyperfine states in the presence of a magnetic field $\mathbf{B}$ in the field-free basis set $\{|vLFSJJ_z\rangle\}$ [10, 11]:

$$|vLnJ_z(\mathbf{B}, 0)\rangle = \sum_{F'S'J'}\beta^{vLnJ_z}_{F'S'J'}(\mathbf{B})|vLF'S'J'J_z\rangle. \tag{38}$$

Note that in Eq. (38) there is no summation over the angular momentum projection J_z, since it remains a good quantum number in a homogeneous magnetic field. The computational advantage of evaluating the electric quadrupole shift $\Delta E_{\rm Q}^{vLnJ_z}$ by diagonalizing the matrix of $V^{\rm Q}$ in Eq. (37) instead of $H_{\rm eff}^{\rm tot+Q}$ is that no precision is lost in the subtraction $E^{vLnJ_z}(\mathbf{B}, Q) - E^{vLnJ_z}(\mathbf{B}, 0)$. Note again that the matrix element in Eq. (37) vanishes for $L = 0$.

4.4 First-order perturbation theory

In first order of perturbation theory, the quadrupole shift is given by the diagonal matrix element of $V^{\rm Q}$,

$$\begin{aligned}\Delta E^{vLnJ_z}_{\rm Q,diag} &= \left\langle vLnJ_z(\mathbf{B},0)|V^{\rm Q}|vLnJ_z(\mathbf{B},0)\right\rangle\\ &= E_{14}\tilde{Q}^0(\mathbf{R}_B)\left\langle vLnJ_z(\mathbf{B},0)|(\mathbf{L}\otimes\mathbf{L})^{(2)}_0|vLnJ_z(\mathbf{B},0)\right\rangle\\ &= E_{14}\langle L||(\mathbf{L}\otimes\mathbf{L})^{(2)}||L\rangle\tilde{Q}^0(\mathbf{R}_B)\\ &\times\sum_{FSJ'J}(-1)^{S+J'+L}\sqrt{2J+1}C^{J'J_z}_{JJ_z,20}\beta^{vLnJ_z}_{FSJ'}(\mathbf{B})\beta^{vLnJ_z}_{FSJ}(\mathbf{B})\\ &\begin{Bmatrix} L & 2 & L\\ J' & S & J\end{Bmatrix}\end{aligned} \tag{39}$$

to which only the longitudinal component $Q_{zz} = \tilde{Q}^0(\mathbf{R}_B)$ of the electric field gradient contributes; since Q_{zz} does not

Table 2 Numerical values of the coefficients E_{14} of the effective Hamiltonian, Eq. (20), for some rovibrational states (v, L) of H_2^+, with units MHz m^2/GV

L	$v = 0$	1	2	3	4	5	6	7	8
0	−0.3018(−3)	−0.3448(−3)	−0.3910(−3)	−0.4409(−3)	−0.4948(−3)	−0.5533(−3)	−0.6172(−3)	−0.6874(−3)	−0.7652(−3)
1	0.1815(−3)	0.2074(−3)	0.2351(−3)	0.2651(−3)	0.2975(−3)	0.3327(−3)	0.3711(−3)	0.4133(−3)	0.4601(−3)
2	0.4343(−4)	0.4960(−4)	0.5624(−4)	0.6340(−4)	0.7115(−4)	0.7956(−4)	0.8873(−4)	0.9883(−4)	0.1100(−3)
3	0.2042(−4)	0.2331(−4)	0.2642(−4)	0.2978(−4)	0.3342(−4)	0.3736(−4)	0.4167(−4)	0.4641(−4)	0.5168(−4)
4	0.1205(−4)	0.1375(−4)	0.1558(−4)	0.1756(−4)	0.1970(−4)	0.2202(−4)	0.2456(−4)	0.2736(−4)	0.3046(−4)
5	0.8022(−5)	0.9151(−5)	0.1037(−4)	0.1168(−4)	0.1310(−4)	0.1464(−4)	0.1633(−4)	0.1819(−4)	0.2026(−4)
6	0.5769(−5)	0.6577(−5)	0.7448(−5)	0.8388(−5)	0.9406(−5)	0.1051(−4)	0.1173(−4)	0.1306(−4)	0.1455(−4)
7	0.4377(−5)	0.4987(−5)	0.5645(−5)	0.6355(−5)	0.7124(−5)	0.7962(−5)	0.8881(−5)	0.9895(−5)	0.1103(−4)
8	0.3456(−5)	0.3935(−5)	0.4452(−5)	0.5010(−5)	0.5615(−5)	0.6275(−5)	0.6999(−5)	0.7800(−5)	0.8698(−5)
9	0.2814(−5)	0.3202(−5)	0.3621(−5)	0.4073(−5)	0.4564(−5)	0.5100(−5)	0.5689(−5)	0.6342(−5)	0.7075(−5)
10	0.2349(−5)	0.2671(−5)	0.3019(−5)	0.3394(−5)	0.3803(−5)	0.4249(−5)	0.4740(−5)	0.5286(−5)	0.5902(−5)

The notation $a(-b)$ stands for $a \times 10^{-b}$. In order to convert the values to atomic units ($e\, a_B^2$), multiply by 1476.87

mix states with different values of J_z, J_z remains a good quantum number in this case. The transversal components that couple states with different values of J_z contribute in second order of perturbation theory only; for the electric and magnetic fields of interest, the second-order effects are below 0.1 Hz and will be neglected in what follows.

We may rewrite the above equation in a simplified notation,

$$\Delta E_{\mathrm{Q,diag}}^{vLFSJJ_z} = \sqrt{\frac{3}{2}} E_{14}(v,L) Q_{zz} \langle vLFSJJ_z | L_z^2 - \frac{1}{3}\mathbf{L}^2 | vLFSJJ_z \rangle. \tag{40}$$

From the property of the 6-j symbols, we see that the shift vanishes if $L = 0$. Furthermore, in the limit of zero magnetic field B,

$$\beta_{FSJ}^{vLnJ_z}(\mathbf{B}) \simeq \beta_{FSJ}^{vLnJ_z}(0) = \delta_{JJ_n} \beta_{FSJ}^{vL(F_nS_nJ_n)J_z}(0). \tag{41}$$

The sum over J, J' in Eq. (39) is then proportional to

$$\begin{Bmatrix} L & L & 2 \\ J & J & S' \end{Bmatrix}.$$

This 6-j symbol vanishes for $J = J_n = 0$ hyperfine levels. Therefore, the shift nearly vanishes for such levels in the limit of small magnetic field. Thus, for example, a transition $(v, L = 0, n, J_z) \to (v', L', n', J_z' = 0)$ such that $J_{n'} = 0$ is nearly free of quadrupole shift if the magnetic field is small. Table 6 below contains such a transition.

4.5 Numerical example

We have performed numerical diagonalization of the effective Hamiltonian Eq. (20), including hyperfine coupling, Zeeman interaction, and quadrupole interaction as described in Sect. 4.2. For example, for the level $(v = 0, L = 1)$ in $B = 1$ G, and a purely longitudinal gradient $Q = Q_{zz} = 10^8$ V/m^2 for a gradient with non-zero transversal components $Q = (\tilde{Q}^{-1} = 100 \times 10^8, \tilde{Q}^0 = 10^8)$ V/m^2, and for $(\tilde{Q}^{-2} = 100 \times 10^8, \tilde{Q}^0 = 10^8)$ V/m^2 the largest relative difference between the "exact" quadrupole shift $\Delta E_{\mathrm{Q}}^{vLnJ_z}$ and the diagonal approximation $\Delta E_{\mathrm{Q,diag}}^{vLnJ_z}$, Eq. (39), is 9×10^{-4}. The maximum absolute deviation is 9×10^{-5} Hz. For concreteness, we have also studied the effect of reducing the magnetic field from 1 G to 0.1 G for the (0,3), (3,4) and (5,4) levels that support some of the metrologically interesting transitions listed in Table 7. All Zeeman states exhibit very small relative and very small absolute differences <0.06 Hz between the full diagonalization value (when $\tilde{Q}_{\pm 2} = \tilde{Q}_{\pm 1} = \tilde{Q}_0$ was set) and the expectation value results (which takes only $\tilde{Q}_0$ into account) also in 0.1 G, except for the $J_z \neq 0$ hyperfine Zeeman states of those two particular hyperfine levels that also contain the particularly favourable $J_z = 0 \to$

Table 3 Numerical values of the coefficients E_{14} of the effective Hamiltonian, Eq. (20), for some rovibrational states (v, L) of D_2^+, with units MHz m^2/GV

L	$v = 0$	1	2	3	4	5	6	7	8
0	−0.2957(−3)	−0.3254(−3)	−0.3568(−3)	−0.3898(−3)	−0.4246(−3)	−0.4613(−3)	−0.5002(−3)	−0.5414(−3)	−0.5852(−3)
1	0.1776(−3)	0.1955(−3)	0.2143(−3)	0.2341(−3)	0.2550(−3)	0.2771(−3)	0.3004(−3)	0.3252(−3)	0.3515(−3)
2	0.4240(−4)	0.4666(−4)	0.5114(−4)	0.5587(−4)	0.6085(−4)	0.6612(−4)	0.7169(−4)	0.7759(−4)	0.8386(−4)
3	0.1986(−4)	0.2185(−4)	0.2395(−4)	0.2616(−4)	0.2849(−4)	0.3096(−4)	0.3356(−4)	0.3632(−4)	0.3926(−4)
4	0.1166(−4)	0.1283(−4)	0.1406(−4)	0.1536(−4)	0.1673(−4)	0.1817(−4)	0.1970(−4)	0.2132(−4)	0.2304(−4)
5	0.7722(−5)	0.8494(−5)	0.9307(−5)	0.1016(−4)	0.1107(−4)	0.1202(−4)	0.1303(−4)	0.1410(−4)	0.1524(−4)
6	0.5515(−5)	0.6065(−5)	0.6645(−5)	0.7255(−5)	0.7900(−5)	0.8580(−5)	0.9301(−5)	0.1006(−4)	0.1088(−4)
7	0.4152(−5)	0.4565(−5)	0.5000(−5)	0.5459(−5)	0.5943(−5)	0.6454(−5)	0.6995(−5)	0.7570(−5)	0.8181(−5)
8	0.3250(−5)	0.3573(−5)	0.3912(−5)	0.4270(−5)	0.4648(−5)	0.5047(−5)	0.5470(−5)	0.5919(−5)	0.6397(−5)
9	0.2622(−5)	0.2881(−5)	0.3155(−5)	0.3442(−5)	0.3746(−5)	0.4068(−5)	0.4408(−5)	0.4769(−5)	0.5154(−5)
10	0.2167(−5)	0.2381(−5)	0.2605(−5)	0.2843(−5)	0.3093(−5)	0.3358(−5)	0.3638(−5)	0.3936(−5)	0.4254(−5)

The notation $a(-b)$ stands for $a \times 10^{-b}$. In order to convert the values to atomic units ($e\,a_B^2$), multiply by 1476.87

$J'_z = 0$ transition with −2.3 Hz Zeeman shift (Table 7). For the $J'_z \neq 0$ states the absolute difference increases from a maximum of 0.4 Hz to a maximum of 2.5 Hz when **B** is reduced to 0.1 G. For the $J'_z = 0$ states it does not exceed 0.25 Hz even in 0.1 G. These differences are related to the small Zeeman splittings in these particular hyperfine levels. However, these differences do not affect the discussion and conclusions below. There is no difference if $\tilde{Q}_0$ is the only nonzero component. Thus, the diagonal approximation produces—within the adopted accuracy—essentially the same numerical values of the quadrupole shift as the full diagonalization of the effective Hamiltonian, except in a few special cases.

4.6 The shift of the stretched states

A special case is the stretched states. For any rovibrational level (v, L), these are the two states with maximum total angular momentum and projection,

$$|vLn_sJ_z(\mathbf{B},0)\rangle = |v, L, F = 1, S = 2, J = L+2, J_z = \pm(L+2)(\mathbf{B},0)\rangle,$$

introduced in Refs. [10, 11]. The expansion Eq. (38) of these for any magnetic field strength contains only a single non-zero coefficient, $\beta_{FSJ}^{vLn_sJ_z=\pm J}(\mathbf{B}) = \delta_{F1}\delta_{S2}\delta_{JL+2}$. Using this, we obtain the simple expression for both stretched states:

$$\Delta E_{\mathrm{Q,diag}}^{vLn_sJ_z=\pm(L+2)}(B) = \frac{L(2L-1)}{\sqrt{6}} E_{14} Q_{zz}. \tag{42}$$

The shift is equal for both stretched states and independent of magnetic field strength.

5 Numerical results for HD^+

5.1 Energy shifts

To illustrate the magnitude of the electric quadrupole shift, we list in Table 4 the quadrupole shifts $\Delta E_{\mathrm{Q,diag}}^{vLnJ_z}(\mathbf{B})$ of the hyperfine energy levels of the initial and final states, $(v=0, L=1)$ and $(v=4, L=2)$, of a particular one-photon rovibrational transition in HD^+, discussed in detail in Ref. [10, 11]. We choose a value $Q_{zz} = 0.1$ GV m^{-2} which could be present in a linear ion trap in which one HD^+ ion and one Be^+ion (for sympathetic cooling and quantum logic interrogation) are located at a few μm distance. Comparison with Table 2 of Refs. [10, 11] shows that the quadrupole shift is typically orders of magnitude smaller than the Zeeman shift. We emphasize that the quadrupole shift of a given hyperfine state does depend on the magnetic field strength, although the dependence is weak for

the majority of the states (at the field value assumed in the Table). It is useful to compare the values with those relevant for a particular atomic ion used for atomic ion clocks: the upper level of the octupole transition of $^{171}Yb^+$ has an electric quadrupole shift of 2 Hz in the same gradient, at a transition frequency of 642 THz [33].

5.2 Metrologically interesting transitions

Since the Zeeman shift is the dominant shift, we have searched for transitions with small Zeeman shifts of the transition frequencies when the magnetic field is moderate (1 G) and report below their electric quadrupole shifts $\Delta f_Q = (\Delta E^{v'L'n'J'_z}_{\mathrm{Q,diag}}(\mathbf{B}) - \Delta E^{vLnJ_z}_{\mathrm{Q,diag}}(\mathbf{B}))/h$. For simplicity, we confined the search to the range $v' \le 5$,[1] implying transition wavelengths larger than approximately 1.1 μm. The search also found transitions with a small Zeeman shift at 1 G which is of spurious origin, the transition not actually being weakly dependent on the magnetic field. Such transitions are not discussed further. This leaves essentially two types of transitions (exceptions are mentioned below):

1. of the type $J_z = 0 \to J'_z = 0$, characterized by a quadratic Zeeman shift, and
2. transitions between stretched states. For any pair of rovibrational levels (v, L), (v', L'), these are the two transitions

$$(v, L, F = 1, S = 2, J = L + 2, J_z = J) \to (v', L', F' = 1, S' = 2, J' = L' + 2, J'_z = J'),$$
$$(v, L, F = 1, S = 2, J = L + 2, J_z = -J) \to (v', L', F' = 1, S' = 2, J' = L' + 2, J'_z = -J').$$

Their favorable metrological properties have been discussed in Refs. [10, 11]. Basically, since the Zeeman shift of the transition doublet is strictly linear, one has the possibility of nulling the effect of the magnetic field by measuring both transition frequencies (at any actual value of the magnetic field) and then computing the average value. However, the electric quadrupole shift is equal for both transitions in the doublet, so no simple cancelation occurs.

5.3 Radio-frequency transitions

Magnetic (M1) hyperfine transitions within rovibrational levels having rotational angular momentum $L = 0$ are free of electric quadrupole shifts. Unfortunately, all M1 transitions in the rovibrational ground state ($v = 0$, $L = 0$), which is well accessible experimentally, have comparatively large Zeeman shifts.

It may be of interest to measure hyperfine transitions in levels with non-zero L, in order to test L-dependent contributions to their frequencies. For this purpose, Table 5 shows a list of transitions between hyperfine states selected with the criterium of less than 0.1 kHz Zeeman shift at 1 G for individual transitions with quadratic Zeeman effect and less than 0.6 kHz shift of the mean frequency of transition pairs. We have included transitions with both small and large RF frequency. No selection was performed with respect to the electric quadrupole shift because the criterium of small Zeeman shifts is regarded as more important for experimental reasons. In the search, we confined ourselves to the range $v = 0$, 1, and $L = 0$, 1, 2 in order to limit the number of results.

We find a substantial number of $J_z = 0 \to J'_z = 0$ transitions with Zeeman shifts of approximately 0.2–0.5 kHz at 1 G. A particularly low Zeeman shift (3 Hz in 1 G, 0.3 Hz in 0.5 G) occurs for the 947.6 MHz hyperfine transition in $(v = 1, L = 1)$. This shift is closely quadratic in B only for $B < 0.4$ G. Since the electric quadrupole shift is also low, −1.1 Hz, the transition is an interesting candidate for a precision test of the hyperfine Hamiltonian. Note, however, that this rovibrational level is an excited one, with finite spontaneous lifetime (55 ms), giving rise to a natural broadening of the transition of 6 Hz. Suppose that we can measure an RF transition frequency with a resolution equal to 1 % of the natural linewidth, i.e. 0.06 Hz. By measuring the transition frequency as a function of the magnetic field, it should be feasible to reduce the Zeeman effect uncertainty to below 0.03 Hz.

Furthermore, a number of transition pairs exist (including in $v = 0$) which have large but nearly opposite Zeeman shifts, with a modest mean shift. Examples with particularly low mean shift, from 2 to 80 Hz at 1 G, are shown in the table. We note that due to the nearly complete cancelation of the opposite shifts, the mean shifts should be considered as indicative only. It should be noted that small magnetic field gradients in the ion trap will cause inhomogeneous broadening of these RF transitions if spectroscopy is performed on ensembles of ions.

5.4 Rotational transitions

The two most easily accessible rotational transitions have been considered in the search, namely the ones occurring in the ground vibrational level $v = 0$ and having the lowest transition frequencies: $(v = 0, L = 0) \to (0, 1)$ at 1.3 THz and $(v = 0, L = 1) \to (0, 2)$ at 2.6 THz. Of these, the 1.3 THz transition has already been observed experimentally [34]. Table 6 reports selected hyperfine components.

[1] Values of the hyperfine Hamiltonian coefficients for $v = 5$ and $L = 5$ levels were computed by V. Korobov and A. Bekbaev (private communication). The rotational g-factors for these levels were extrapolated from those of lower levels.

Table 4 Quadrupole shifts $\Delta E_{\mathrm{Q}}^{vLnJ_z}(B)$ (in Hz) of the hyperfine states $n = (FSJ)$ in the $(v, L) = (4, 2)$ (top) and (0, 1) (bottom) rovibrational states of HD^+

State	J_z								
(FSJ)	−4	−3	−2	−1	0	1	2	3	4
(124)	**17.5**	5.8	−3.3	−9.5	−12.4	−11.6	−6.7	2.9	**17.5**
		17.5	0.4	−10.1	−14.0	−10.8	−0.4	17.5	
(113)		17.5	0.2	−10.3	−14.0	−10.6	−0.2	17.5	
(123)		2.9	−1.2	−3.3	−3.6	−2.1	1.1	5.9	
			8.3	−4.0	−8.7	−4.7	9.2		
(102)			16.0	−8.0	−16.1	−8.0	16.1		
(112)			9.6	−3.8	−9.7	−5.8	9.9		
(122)			−3.8	1.7	3.3	1.6	−2.8		
(011)				5.4	−12.2	6.8			
(111)				4.2	−10.9	6.5			
(121)				−5.9	10.9	−5.0			
(120)					0.05				
State	J_z								
(FSJ)		−3	−2	−1	0	1	2	3	
(123)		**7.9**	−4.9	−7.5	−5.6	−1.5	3.2	**7.9**	
(012)			7.9	−3.4	−7.8	−4.5	7.9		
(112)			7.9	−3.8	−7.9	−4.1	7.9		
(122)			−3.0	6.6	7.2	0.8	−11.1		
(011)				−4.5	7.8	−3.4			
(101)				6.6	−13.1	6.6			
(111)				−2.5	4.6	−2.2			
(121)				0.6	−0.9	0.4			
(010)					0.02				
(110)					0.02				

The magnetic field is $B = 1$ G and the electric field gradient has its only non-vanishing component along the magnetic field $Q = \tilde{Q}^0 = Q_{zz} = 0.1\ \mathrm{GV\,m^{-2}}$, with the only non-vanishing component along the magnetic field. The underlined numbers correspond to hyperfine states with $J = 0$, for which the quadrupole shift vanishes in the limit of vanishing magnetic field. The bold numbers correspond to stretched states

For each of the two cases $\Delta J_z = 0$ and $\Delta J_z = \pm 1$ those transitions having lowest absolute Zeeman shift $|\Delta f_B|$ in a magnetic field of 1 G are listed. The transitions in $(v = 0, L = 0) \rightarrow (0, 1)$ have comparatively large Zeeman shifts, leaving as the most interesting transitions the "stretched-state" doublet at 10.1 MHz, whose two components have equal and opposite Zeeman shift and for which the electric quadrupole shift is 7.9 Hz in a 10^8 V/m^2 field gradient. The second rotational transition listed, $(v = 0, L = 1) \rightarrow (0, 2)$, contains one hyperfine component with a particularly small quadratic second-order Zeeman shift (9 Hz at 1 G) and moderate electric quadrupole shift (−13.5 Hz). By a careful measurement of the absolute frequency shift of this transition as a function of applied magnetic field, it appears possible to achieve an uncertainty of the Zeeman shift equal to 0.2 % of the value at 1 G, or approximately 0.04 Hz (2×10^{-14} relative to the absolute transition frequency).

5.5 Rovibrational transitions

The search for favorable rovibrational transitions was limited to transitions originating in $v = 0, 1$ and ending in $v' \leq 5$. A subset of transitions was selected according to the criterium that their Zeeman shifts are less than 60 Hz for fields less than 1 G. The transitions orginating from $v = 1$ do not offer any advantages compared to those orginating from the ground vibrational state, and we limit the following discussion to the latter. They are shown in Table 7. These are all $J_z = 0 \rightarrow J_z' = 0$ transitions. Two transitions (at −16.0 and 71.1 MHz) have particularly low Zeeman shifts, 6 and −2 Hz at 1 G, respectively. The small differential Zeeman shifts do not arise

Table 5 Systematic shifts of selected radio-frequency M1 transitions $(v, L, F, S, J, J_z) \to (v, L, F', S', J', J'_z)$ (lower → upper)

(v, L)	F'	S'	J'	J'_z	F	S	J	J_z	f_0 (1 G) (MHz)	Rel. int.	Δf_B (1 G) (Hz)	Δf_Q (1 G) (Hz)	$(\Delta E_Q)_u$ (Hz)	$(\Delta E_Q)_l$ (Hz)	$\Delta\alpha^{(t)}$ (at.u.)	$\Delta\alpha^{(l)}$ (at.u.)
(0, 1)	1	2	1	0	0	1	0	0	969	0.787	422	−1.0	−0.9	0.0	7.1	−14.1
(0, 2)	1	2	1	−1	1	0	2	−2	184.1	0.004	−1340044	−13.7	−3.6	10.1	33.1	−66.1
(0, 2)	1	2	1	1	1	0	2	2	186.8	0.003	1339960	−13.3	−3.1	10.1	33.1	−66.1
(0, 2)	1	2	2	0	1	1	3	0	97.3	0.029	−150	11.1	2.1	−9.0	−27.2	54.3
(0, 3)	1	1	4	−4	0	1	3	−3	906.7	0.201	−1082845	3.4	13.2	9.8	−4.0	7.9
(0, 3)	1	1	4	4	0	1	3	3	908.9	0.202	1082924	3.2	13.2	10.0	−4.0	7.9
(0, 3)	1	2	3	0	1	1	4	0	93.5	0.025	446	5.8	−3.6	−9.4	−7.0	14.1
(1, 1)	1	2	1	1	0	1	0	0	948.8	0.641	1192371	0.4	0.5	0.0	−4.3	8.6
(1, 1)	1	2	1	−1	0	1	1	0	950.5	0.113	−1192392	−8.1	0.7	8.8	64.0	−128
(1, 1)	1	2	1	0	0	1	0	0	947.6	0.784	3	−1.1	−1.1	0.0	8.6	−17.2
(1, 2)	1	2	2	0	1	1	3	0	95.9	0.028	−297	12.5	2.3	−10.1	−31.8	63.5
(1, 3)	1	2	3	2	1	1	4	3	92.1	0.026	−121796	−3.7	0.0	3.7	4.6	−9.3
(1, 3)	1	2	3	−2	1	1	4	−3	92.4	0.025	121798	−3.8	0.0	3.8	4.6	−9.3
(1, 3)	1	1	4	4	0	1	3	3	887	0.204	1078708	3.6	14.8	11.3	−4.6	9.2
(1, 3)	1	1	4	−4	0	1	3	−3	884.9	0.202	−1078713	3.8	14.8	11.0	−4.6	9.2
(1, 3)	1	2	3	0	1	1	4	0	92.2	0.025	315	6.6	−4.0	−10.6	−8.2	16.4

f_0 is the transition frequency (excluding the quadrupole shift, including Zeeman shift for 1 Gauss). l, u refers to the lower and upper state, respectively. The intensity of a transition is normalized to the strongest radio-frequency transition having the same value of $|J_z - J'_z|$ and in the same rovibrational level. Δf_B denotes the Zeeman shift of the transition frequency in a magnetic field of 1 G; $\Delta f_Q = (\Delta E_Q)_u - (\Delta E_Q)_l$ is the electric quadrupole shift of the transition in a field gradient $Q_{zz} = 10^8$ V/m^2, while $(\Delta E_Q)_l$, $(\Delta E_Q)_u$ are the electric quadrupole shifts of the lower and upper states, respectively, here given in Hz. $\Delta\alpha^{(t)} = (\alpha^{(t)})_u - (\alpha^{(t)})_l$, $\Delta\alpha^{(l)} = (\alpha^{(l)})_u - (\alpha^{(l)})_l$ are the transverse and longitudinal differential electric polarizabilities between upper and lower state, respectively, in atomic units and in 1 G magnetic field. The near-zero quadrupole shift in the state ($v = 1$, $L = 3$, $F = 1$, $S = 2$, $J = 3$, $J_z = \pm 2$) is a coincidence

from strong cancellation of large individual shifts, but from cancellation of moderate shifts: For example, the −2.3 Hz shift results from individual shifts of 58 Hz and 60 Hz, while the 6.3 Hz shift from two individual shifts of approximately 6.2 kHz. The latter represents the largest relative cancellation of all transitions in Table 7, and is still consistent with the nonrelativistic approximations inherent in the Zeeman shift calculation. If it is possible to minimize the magnetic field in the trap, e.g. to 0.02 G, the quadratic Zeeman shift is reduced by a factor $\simeq 2500$, to a fractional level of approx. 2×10^{-17} and 4×10^{-18}, respectively. This is a negligible shift compared to the other systematic effects discussed here. The electric quadrupole shift of these transitions is approx. -3×10^{-14} at the given gradient value.

Another transition worth noting is the $(1, 0, 1, 0) \to (1, 0, 2, 0)$ transition in $(v = 0, L = 1) \to (2, 2)$ (not shown in Table 7), which has $\Delta f_B = 102.5$ Hz at 1 G, and one of the lowest fractional electric quadrupole shifts, $\Delta f_Q = 0.26$ Hz (2.3×10^{-15}). The relatively large Zeeman shift at 1 G would be reduced to the 4×10^{-16} level in a 0.02 G field.

If, however, the magnetic field is at the 1 G level, for which the Zeeman shift is appreciable, one may determine the shift precisely by measuring the frequency shift of the transition as a function of applied magnetic field. Suppose that the transition frequency can be measured with a resolution equal to 1 % of the natural linewidth at each magnetic field value, e.g., 0.14 Hz for a transition $v = 0 \to v' = 3$. The result of the Zeeman shift evaluation may then reach an uncertainty of 0.04 Hz or 2×10^{-16} relative to the absolute transition frequency of this overtone transition.

A second set of transitions are the stretched-state doublets, tabulated in Table 8. For space reasons, we have not included transitions to $v' = 5$ or $L' = 5$ levels. Their linear Zeeman shift is approximately ±0.5 kHz/G. Suppose that each transition frequency of a doublet can be measured with a resolution equal to 1 % of the natural linewidth, e.g. 0.14 Hz for the transition $v = 0 \to v = 3$. Then, the Zeeman effect uncertainty of the mean of the doublet frequencies would be 0.2 Hz, or approximately 1×10^{-15} relative to the absolute transition frequency. Repeating this for a set of magnetic field values could reduce the error to 2×10^{-16}. The electric quadrupole shift of this particular transition is one order of magnitude smaller than the typical shift of all other stretched-state transitions, −0.3 Hz versus several Hz, or 2×10^{-15} relative to the absolute transition frequency.

5.6 Two-photon rovibrational transitions

Two-photon transitions (E2) are of interest since they can be excited with suppression of first-order Doppler shift even

Table 6 Systematic shifts of selected rotational transitions in the vibrational ground state $v = 0$

(v', L') upper	(v, L) lower	F'	S'	J'	J'_z	F	S	J	J_z	Freq.(1 G) (MHz)	Rel. int.	Δf_B (1 G) (Hz)	Δf_Q (1 G) (Hz)	$(\Delta E_Q)_u$ (Hz)	$(\Delta E_Q)_l$ (Hz)	$\Delta\alpha^{(t)}$ (at.u.)	$\Delta\alpha^{(l)}$ (at.u.)
(0, 1)	(0, 0)	0	1	1	0	0	1	1	0	1.7	0.002	−867	7.8	7.8	0	−449.7	−274.5
(0, 1)	(0, 0)	1	2	1	0	1	2	2	0	−33.2	0.42	−2780	−0.9	−0.9	0	−384.2	−405.4
(0, 1)	(0, 0)	0	1	2	0	0	1	1	0	−2.1	0.755	−2915	−7.8	−7.8	0	−332.9	−508.2
(0, 1)	(0, 0)	0	1	0	0	0	1	1	0	6.1	0.377	3818	0.0	0.0	0	−391.3	−391.3
(0, 1)	0, 0)	1	0	1	0	1	0	0	0	−9.1	1	5050	−13.1	−13.1	0	−293.7	−586.5
(0, 1)	(0, 0)	1	1	2	0	1	1	1	0	11.8	0.756	−6171	−7.9	−7.9	0	−332.8	−508.3
(0, 1)	(0, 0)	1	2	3	±3	1	2	2	±2	10.1	1	∓558	7.9	7.9	0	−449.8	−274.3
(0, 2)	(0, 1)	0	1	2	0	0	1	1	0	0.2	0.798	9	−13.5	−5.6	7.8	72.2	−144.4
(0, 2)	(0, 1)	0	1	3	0	0	1	2	0	−2.1	0.957	792	−1.2	−9.0	−7.8	−36.3	72.7
(0, 2)	(0, 1)	0	1	1	0	0	1	0	0	1.8	0.886	−840	−7.9	−7.9	0.0	19.3	−38.6
(0, 2)	(0, 1)	1	2	4	±4	1	2	3	±3	12.9	1	∓558	3.4	11.3	7.9	30.9	−61.7

An entry having two signs for J_z and J'_z indicates the two transitions between stretched states. The frequency value is the spin-dependent contribution to the total transition frequency f_0. For the $(0,0) \to (0,1)$ transition, $f_0 \simeq 1.3$ THz. For the $(0,1) \to (0,2)$ transition, $f_0 \simeq 2.6$ THz. The intensity of each transition is normalized to that of the strongest transition of the particular rotational transition having the same $|\Delta J_z|$. Other notations are as in Table 5

without strong spatial confinement of the ions. These transitions were discussed for HD^+ in Ref. [13]. It was subsequently shown in Ref. [9] that there exist two-photon transitions without any Zeeman shift as well as stretched-state transitions. Table 9 reports two-photon transitions between levels having low values of L and L'. These are favorable from the experimental point of view, since the number of two-photon transitions arising from a pair of levels is reduced when the angular momenta are small, which translates in a higher transition strength per transition. Also, populating sufficiently strongly the lower hyperfine state is simplified.

The most favorable transition from the point of view of the systematic shifts due to magnetic field and electric field gradient is the stretched-state transition of $(v = 0, L = 0) \to (v' = 2, L' = 0)$, as both effects are absent. The stretched-state transition of $(0, 1) \to (2, 1)$ is also advantageous. For the latter, assuming the same criterium as above, the Zeeman effect uncertainty would be 0.03 Hz, or approximately 3×10^{-16} relative to the absolute two-photon transition frequency. The electric quadrupole shift is 2 Hz, nearly two orders larger.

6 Discussion

6.1 Quadrupole shift measurement and cancelation

The previous section has shown that among the rovibrational transitions having small Zeeman shifts (Tables 7, 8), the electric quadrupole shifts range from absolute values of zero to approximately 10 Hz, in a typical gradient of 10^8 V/m^2. For those transitions for which the shift is finite (i.e. excluding the particular two-photon transitions), the relative values range from $\simeq 1 \times 10^{-15}$ to the largest values $\simeq 1 \times 10^{-13}$ in fractional units. It is useful to compare these magnitudes with the value for atomic ions used in ion optical clocks. For example, in the mercury ion, the shift is on the order of 10 Hz for the same gradient strength, or 1×10^{-14} in relative units [35].

Although small for selected transitions of HD^+, the quadrupole shift can actually be determined and nulled. The property that the electric quadrupole shift depends only on the component of the gradient tensor in the direction of the magnetic field allows for a determination and cancelation of the quadrupole shift. The approach is similar to one of the methods of quadrupole shift control applied to atomic ions in ion optical clocks, introduced by Itano [35].

Consider applying the magnetic field in turn along three orthogonal spatial directions x, y, z, and measuring the corresponding transition frequencies f_x, f_y, f_z, keeping the magnetic field strength constant. Since $f_i = f_0 + (\Delta f_Q)_i$, $i = x, y, z$, and the transition frequency shift is linear in the gradient strength, $(\Delta f_Q)_i = pQ_{ii}$, where $p = p(v, L, n, J_z, v', L', n', J'_z$, is the sensitivity of the particular transition frequency, we have

$$\begin{aligned} f_x &= f_0 + pQ_{xx}, \\ f_y &= f_0 + pQ_{yy}, \\ f_z &= f_0 + pQ_{zz}. \end{aligned} \tag{43}$$

Since the gradients satisfy the Laplace equation $Q_{xx} + Q_{yy} + Q_{zz} = 0$, we obtain

Table 7 Selected rovibrational transitions with small quadratic Zeeman shifts at 1 G

(v', L') upper	(v, L) lower	F'	S'	J'	J'_z	F	S	J	J_z	freq.(1 G) (MHz)	rel. int.	Δf_B (1 G) (Hz)	Δf_Q (1 G) (Hz)	$(\Delta E_Q)_u$ (Hz)	$(\Delta E_Q)_l$ (Hz)	$\Delta\alpha^{(t)}$ (at.u.)	$\Delta\alpha^{(l)}$ (at.u.)
(1, 5)	(0, 4)	0	1	5	0	0	1	4	0	16.8	0.97	29.5	−1.6	−10.5	−8.8	−0.5	3.4
(1, 5)	(0, 4)	1	2	5	0	1	2	4	0	−3.1	0.9	−57.3	−2.3	−8.5	−6.2	0.4	1.6
(2, 4)	(0, 3)	0	1	4	0	0	1	3	0	31.8	0.96	24.0	−3.1	−11.1	−7.9	0.5	4.0
(2, 4)	(0, 3)	0	1	5	0	0	1	4	0	30.7	0.99	31.7	−2.7	−12.2	−9.5	−0.5	6.0
(2, 5)	(0, 4)	0	1	5	0	0	1	4	0	32.0	0.97	−38.9	−2.9	−11.7	−8.8	1.1	2.8
(2, 5)	(0, 4)	0	1	6	0	0	1	5	0	31.2	1	−39.6	−2.7	−12.4	−9.7	0.9	3.4
(3, 2)	(0, 1)	1	1	3	0	1	1	2	0	−3.8	0.95	21.2	−4.7	−12.6	−7.9	−20.8	49.6
(3, 3)	(0, 2)	0	1	4	0	0	1	3	0	44.7	0.98	−12.4	−4.2	−13.2	−9.0	−1.5	11.1
(3, 3)	(0, 2)	1	0	3	0	1	0	2	0	−10.8	1	54.8	−3.8	−13.9	−10.1	−3.3	14.7
(3, 4)	(0, 3)	1	2	4	0	1	2	3	0	−16.0	0.84	6.4	−5.0	−8.6	−3.6	5.2	−2.0
(3, 4)	(0, 3)	1	1	5	0	1	1	4	0	−8.4	0.99	−11.2	−4.1	−13.5	−9.4	2.0	4.3
(3, 4)	(0, 3)	0	1	4	0	0	1	3	0	45.9	0.96	−55.0	−4.4	−12.3	−7.9	2.9	2.5
(4, 2)	(0, 1)	0	1	1	0	0	1	0	0	59.1	0.87	−17.7	−12.2	−12.2	0.0	39.8	−67.5
(4, 2)	(0, 1)	0	1	3	0	0	1	2	0	57.5	0.94	−36.7	−6.1	−14.0	−7.8	−13.5	39.1
(4, 3)	(0, 2)	0	1	3	0	0	1	2	0	58.9	0.91	−37.2	−6.7	−12.3	−5.6	7.7	−3.2
(4, 5)	(0, 4)	1	1	4	0	1	1	3	0	−11.4	0.98	−21.1	−5.6	−14.8	−9.1	5.4	1.8
(4, 5)	(0, 4)	1	2	3	0	1	2	2	0	−16.1	0.96	−29.0	−5.7	−13.9	−8.2	5.6	1.3
(4, 5)	(0, 4)	1	2	7	0	1	2	6	0	−24.8	0.98	−30.8	−5.5	−14.8	−9.3	5.3	1.9
(4, 5)	(0, 4)	1	1	5	0	1	1	4	0	−11.9	0.98	−34.3	−5.6	−14.7	−9.2	5.4	1.9
(4, 5)	(0, 4)	0	1	4	0	0	1	3	0	59.0	0.99	−52.6	−5.6	−15.1	−9.5	5.3	1.9
(5, 4)	(0, 3)	0	1	3	0	0	1	2	0	71.1	0.98	−2.3	−7.2	−16.3	−9.1	8.9	−0.2
(5, 5)	(0, 4)	0	1	4	0	0	1	3	0	70.8	0.99	45.9	−7.2	−16.7	−9.5	8.3	1.4

For the $(0,3) \to (2,4)$ transition, the absolute frequency $f_0 \simeq 116$ THz, for the $(0,2) \to (3,3)$ transition, $f_0 \simeq 166$ THz, for the $(0,1) \to (4,2)$ transition, $f_0 \simeq 214$ THz, and for the $(0,3) \to (5,4)$ transition, $f_0 \simeq 261$ THz. See caption of Table 6 for explanations

$$f_0 = \frac{1}{3}(f_x + f_y + f_z),$$
$$pQ_{xx} = \frac{1}{3}(2f_x - f_y - f_z),$$
$$pQ_{yy} = \frac{1}{3}(2f_y - f_x - f_z). \quad (44)$$

The unperturbed transition frequency f_0 is calculated from a simple average over three directions. The error in determining it arises from (1) the uncertainty of each measurement f_x, f_y, f_z and (2) the inaccuracy in establishing three perfectly orthogonal magnetic field directions and thus obtaining a perfect cancelation of the quadrupole shift.

The first uncertainty may be estimated as previously by the 1 % assumption, giving 0.14 Hz/$\sqrt{3}$ for rovibrational transitions $v = 0 \to 3$. The second uncertainty, in a precision experiment on the mercury ion clock, was less than 5×10^{-17} [36]. We may expect that it will eventually be possible to achieve an equivalent uncertainty of this type also for HD^+, that is, in the range between 5×10^{-18} and 5×10^{-16}, depending on the transition (rescaling by the sensitivity of HD^+ compared to Hg^+). Then, the electric quadrupole shift nulling uncertainty for all considered E1 rovibrational transitions will be dominated by the type-(i)-uncertainty. With the 1 % criterium used here, this uncertainty would be approximately 0.5 to 1×10^{-15}, limited by the natural lifetime of the upper level.

Note that since p is known, the gradient strengths can also be determined experimentally, via Eq. (44).

6.2 Other systematic effects

The discussion has so far concentrated on the electric quadrupole shift and the Zeeman shift in a time-independent (d.c.) magnetic field. Other systematic effects affecting transition frequencies of trapped ions are the second-order Doppler shift, the Zeeman shift due to a.c. magnetic fields of the trap, the light shifts, the black-body radiation shift, and the quadratic Stark shift due to stray electric fields of the trap. We comment only on the latter two, since we believe that the others are negligible, with the possible exception of the light shift in case of two-photon transitions. The black-body radiation shift at 300 K is of order 1×10^{-16} for the transitions discussed here [14]. By an accurate determination of the environment temperature or

Table 8 Rovibrational transitions between stretched hyperfine states

(v', L') upper	(v, L) lower	F'	S'	J'	J'_z	F	S	J	J_z	freq.(1 G) (MHz)	rel. int.	Δf_B (1 G) (Hz)	Δf_Q (1 G) (Hz)	$(\Delta E_Q)_u$ (Hz)	$(\Delta E_Q)_l$ (Hz)	$\Delta\alpha^{(t)}$ (at.u.)	$\Delta\alpha^{(l)}$ (at.u.)
(1, 0)	(0, 1)	1	2	2	± 2	1	2	3	± 3	−17.0	1	± 558.3	−7.9	0	7.9	517.2	341.7
(1, 1)	(0, 0)	1	2	3	± 3	1	2	2	± 2	2.6	1	∓ 553.7	8.9	8.8	0	−459.0	−253.8
(1, 1)	(0, 2)	1	2	3	± 3	1	2	4	± 4	−20.4	1	± 562.6	−2.4	8.8	11.3	−40.1	82.2
(1, 2)	(0, 1)	1	2	4	± 4	1	2	3	± 3	4.8	1	∓ 548.9	4.8	12.7	7.9	26.9	−51.7
(1, 2)	(0, 3)	1	2	4	± 4	1	2	5	± 5	−21.6	1	± 566.6	−0.6	12.7	13.2	−15.6	33.4
(1, 3)	(0, 2)	1	2	5	± 5	1	2	4	± 4	4.6	1	∓ 543.8	3.6	14.9	11.3	9.8	−17.4
(1, 3)	(0, 4)	1	2	5	± 5	1	2	6	± 6	−22.3	1	± 570.5	0.3	14.9	14.6	−7.6	17.3
(1, 4)	(0, 3)	1	2	6	± 6	1	2	5	± 5	3.8	1	∓ 538.4	3.1	16.3	13.2	4.8	−7.3
(2, 0)	(0, 1)	1	2	2	± 2	1	2	3	± 3	−23.5	1	± 558.3	−7.9	0	7.9	595.2	419.7
(2, 1)	(0, 0)	1	2	3	± 3	1	2	2	± 2	−4.4	1	∓ 548.9	9.9	9.9	0	−469.6	−230.0
(2, 1)	(0, 2)	1	2	3	± 3	1	2	4	± 4	−27.4	1	± 567.4	−1.4	9.9	11.3	−50.6	106.0
(2, 2)	(0, 1)	1	2	4	± 4	1	2	3	± 3	−2.9	1	∓ 539.1	6.3	14.2	7.9	22.5	−40.1
(2, 2)	(0, 3)	1	2	4	± 4	1	2	5	± 5	−29.3	1	± 576.4	0.9	14.2	13.2	−20.1	44.9
(2, 3)	(0, 2)	1	2	5	± 5	1	2	4	± 4	−3.7	1	∓ 529.1	5.3	16.6	11.3	7.7	−10.5
(2, 3)	(0, 4)	1	2	5	± 5	1	2	6	± 6	−30.6	1	± 585.2	2.1	16.6	14.6	−9.8	24.2
(2, 4)	(0, 3)	1	2	6	± 6	1	2	5	± 5	−5.2	1	∓ 518.8	5.0	18.3	13.2	3.8	−2.6
(3, 0)	(0, 1)	1	2	2	± 2	1	2	3	± 3	−29.5	1	± 558.3	−7.9	0	7.9	685.9	510.4
(3, 1)	(0, 0)	1	2	3	± 3	1	2	2	± 2	−10.9	1	∓ 543.7	11.0	11.0	0	−481.8	−202.4
(3, 1)	(0, 2)	1	2	3	± 3	1	2	4	± 4	−33.9	1	± 572.6	−0.3	11.0	11.3	−62.9	133.6
(3, 2)	(0, 1)	1	2	4	± 4	1	2	3	± 3	−10.1	1	∓ 528.7	7.9	15.8	7.9	17.4	−26.7
(3, 2)	(0, 3)	1	2	4	± 4	1	2	5	± 5	−36.5	1	± 586.8	2.5	15.8	13.2	−25.2	58.4
(3, 3)	(0, 2)	1	2	5	± 5	1	2	4	± 4	−11.6	1	∓ 513.4	7.2	18.5	11.3	5.3	−2.4
(3, 3)	(0, 4)	1	2	5	± 5	1	2	6	± 6	−38.5	1	± 600.9	3.9	18.5	14.6	−12.1	32.2
(3, 4)	(0, 3)	1	2	6	± 6	1	2	5	± 5	−26.2	1	∓ 497.7	7.1	20.3	13.2	2.7	2.8
(4, 0)	(0, 1)	1	2	2	± 2	1	2	3	± 3	−35.2	1	± 558.3	−7.9	0	7.9	791.8	616.3
(4, 1)	(0, 0)	1	2	3	± 3	1	2	2	± 2	−17.0	1	∓ 538.1	12.2	12.2	0	−496.0	−170.0
(4, 1)	(0, 2)	1	2	3	± 3	1	2	4	± 4	−40.0	1	± 578.1	0.9	12.2	11.3	−77.1	165.9
(4, 2)	(0, 1)	1	2	4	± 4	1	2	3	± 3	−16.8	1	∓ 517.6	9.6	17.5	7.9	11.5	−11
(4, 2)	(0, 3)	1	2	4	± 4	1	2	5	± 5	−43.2	1	± 597.9	4.2	17.5	13.2	−31.1	74.1
(4, 3)	(0, 2)	1	2	5	± 5	1	2	4	± 4	−18.9	1	∓ 496.6	9.2	20.5	11.3	2.6	7.0
(4, 3)	(0, 4)	1	2	5	± 5	1	2	6	± 6	−45.8	1	± 617.7	5.9	20.5	14.6	−14.8	41.6
(4, 4)	(0, 3)	1	2	6	± 6	1	2	5	± 5	−21.7	1	∓ 475.2	9.3	22.5	13.2	1.6	9.1

The double sign refers to the pair of transitions $J_z = J \rightarrow J'_z = J'$ and $J_z = -J \rightarrow J'_z = -J'$, which have opposite Zeeman shifts, but the same electric quadrupole shift. The absolute transition frequencies are similar to those of Table 7. See caption of Table 6 for explanations

Table 9 Selected two-photon transitions with favorably low Zeeman shifts

(v', L') upper	(v, L) lower	F'	S'	J'	J'_z	F	S	J	J_z	Freq.(1 G) (MHz)	Rel. int.	Δf_B (Hz)	Δf_Q (1 G) (Hz)	$(\Delta E_Q)_u$ (Hz)	$(\Delta E_Q)_l$ (Hz)	$\Delta\alpha^{(t)}$ (at.u.)	$\Delta\alpha^{(l)}$ (at.u.)
(2,0)	(0,0)	1	2	2	±2	1	2	2	±2	−13.4	1	0	0	0	0	145.4	145.4
(2,2)	(0,0)	1	2	4	±4	1	2	2	±2	7.2	1	∓1096	14.2	14.2	0	−427.3	−314.4
(2,1)	(0,1)	1	2	3	±3	1	2	3	±3	−14.4	1	±10	2.0	9.9	7.9	−19.8	44.3

Each line is a stretched-state doublet. The absolute transition frequencies are $f_0 \simeq 112, 112, 115$ THz, respectively. See caption of Table 6 for explanations

by use of a cryogenic ion trap the uncertainty of this shift can be reduced further by at least one order.

The Stark frequency shift of a transition frequency is given by $\Delta E_S = -(\Delta\alpha^{(l)}E_z^2 + \Delta\alpha^{(t)}(E_x^2 + E_y^2))/2$, where E_x, E_y, E_z are the components of the electric field, and $\Delta\alpha^{(l)}, \Delta\alpha^{(t)}$ are, respectively, the differences of the longitudinal and transverse polarizabilities between upper and lower quantum state. The polarizabilities of the hyperfine states of HD^+ have been calculated in Ref. [15] in the absence of electric quadrupole interaction and for zero magnetic field B, employing the Born–Oppenheimer approximation. A summation method was used, where excited electronic states were negelected. The method is also applicable if the magnetic field is finite. The polarizabilities α of the hyperfine states typically lie in the range of 1–100 atomic units, except for $(v, L = 0)$ levels, where they are 400 atomic units or larger. The work put into evidence the strong variation of the polarizability between different hyperfine state belonging to the same rovibrational level. The hyperfine-state dependence arises in the difference $\Delta\alpha^{(l)} - \Delta\alpha^{(t)}$, while the combination $\Delta\alpha^{(l)} + 2\Delta\alpha^{(t)}$ is independent of the upper and lower hyperfine states. The (normalized) hyperfine-state dependence is precisely obtained from the summation method, but the magnitudes of the two polarizabilities are only accurate at a level of a few at.u.[2] A more accurate calculation is described in [37], based on precise variational wave functions, which include the contribution of excited electronic levels. We use the results of this latter calculation here, which are reported in the tables above. The values from the two calculation approaches differ by an amount that scales with the change in vibrational quantum number and reaches several atomic units for the transitions with $v = 0 \to v' = 4$. The dependence of $\Delta\alpha^{(l)}, \Delta\alpha^{(t)}$ on the magnetic field is very small (<0.1 at.u. between 0 and 1 G) for most transitions in the tables; only for a few, it is on the order 1 at.u.

According to the tables, many transitions exhibit a differential polarizability on the order 10 at.u., which corresponds to a frequency shift coefficient $\Delta E_S/\langle E^2\rangle = 1.2\,\mathrm{mHz/(V/cm)^2}$. We may compare this with the coefficients of atomic ions used in ion clocks. For example, it is 0.14 $\mathrm{mHz/(V/cm)^2}$ for Al^+ and 1 $\mathrm{mHz/(V/cm)^2}$ for the octupole transition in $^{171}Yb^+$. For the latter ion, the associated fractional frequency uncertainty in current state-of-the-art clocks is at the level of less than 10^{-17}, i.e. less than 10 mHz absolute [33]. We assume for the following that it should be possible to reach a similar absolute level, 10 mHz, also for HD^+, if the transitions have a polarizability of 10 a.u., and correspondingly more if the polarizability is higher.

[2] In addition to the neglect of excited electronic states, the calculations in Ref. [15] were performed taking into account only intermediate states with $0 \le v \le 4$. Therefore, the polarizabilities of the $v = 4$, $L = 2$ level given in that paper deviate from the "correct" (within the chosen approximation) values by up to 1 at.u.

6.3 Potential of promising transitions

For the rotational and radiofrequency transitions the relative uncertainties originating from the Stark shift will generally be larger than for the rovibrational transitions due to the smaller transition frequencies.

For the radiofrequency transitions, the differential polarizabilities vanish for $L = 0$ levels, since for these levels, the state polarizabilities are equal for all hyperfine states. The other transitions considered in Table 5 have small or moderate differential polarizabilities. The 947.6 MHz radiofrequency transition in (1, 1) considered in Sect. 5.3 exhibits the differential polarizabilities $\Delta\alpha^{(t)} \simeq 9$ at.u., $\Delta\alpha^{(l)} \simeq -17$ at.u. Following the argument given in the previous paragraph, the corresponding uncertainty should be controllable at the 0.015 Hz level. The electric quadrupole shift should be determinable to about the same level, see Sect. 6.1 and the Zeeman shift inaccuracy was estimated at 0.03 Hz. Thus, in this particular radiofrequency transition, the combined Zeeman, quadrupole, and Stark systematic shift should be controllable to approximately 0.05 Hz uncertainty, or 5×10^{-11} in relative terms.

For the rotational transitions in Table 6, we find polarizabilities ranging from intermediate to large. We estimate that for the stretched-state transition of $(0, 0) \to (0, 1)$ the total systematic shift uncertainty could be 0.5 Hz (5×10^{-13}), whereas it could be 0.15 Hz for the 0.2 MHz component of $(0, 1) \to (0, 2)$, or 5×10^{-14}.

For the one-photon rovibrational transitions, Table 7 contains several with small differential polarizabilities. For example, the –16 MHz hyperfine component of $(0, 3) \to (3, 4)$ and the −71 MHz hyperfine component of $(0, 3) \to (5, 4)$, both of which have negligible Zeeman shift in a 0.02 G magnetic field, would have approximately 0.01 Hz Stark shift uncertainty, less than the one expected from the quadrupole shift, (0.1 Hz). The total uncertainty, $(4–5) \times 10^{-16}$, would be dominated by the latter.

Among the stretched-state rovibrational one-photon transitions in Table 8 there are several that have differential polarizabilities of 10 at.u. or less and therefore contribute much less to the total uncertainty than the Zeeman effect and the electric quadrupole effect. Here, too, a total uncertainty of 5×10^{-16} appears possible.

Finally, for the two-photon transitions in Table 9, the differential polarizabilities are moderate to large. For the $(0, 0) \to (2, 0)$ transition, the Stark effect is the only non-zero systematic effect of the three types considered. Its contribution

to the transition frequency uncertainty would be 0.14 Hz according to our assumptions, or 1×10^{-15} in relative terms. A rough estimate of the light shift is 1 Hz (1×10^{-14}). Thus, this shift must be measured to the sub-10 % level in order to reduce the total uncertainty to 1×10^{-15}.

7 Conclusion

In this paper, we have developed an exact treatment of the interaction of molecular hydrogen ions with a static electric quadrupole field. This was simplified by applying the Born–Oppenheimer approximation and we derived an approximate effective Hamiltonian. We computed the corresponding coupling coefficients E_{14} for the three non-radioactive molecular hydrogen ion species. The quadrupole shift can be obtained with sufficient accuracy by applying first-order perturbation theory. It is worth noting that the computational scheme outlined here may be useful in estimating similar effects in the spectroscopy of exotic bound systems (such as muonic hydrogen molecular ions [38, 39]) in the liquid or solid phase. The shift of energy levels with zero rotational angular momentum vanishes. Experimentally, the quadrupole shift can be nulled by measuring the mean of the transition frequencies when the magnetic field is aligned along three orthogonal directions. This holds true for all molecular hydrogen ions and is due to the smallness of the quadrupole interaction.

We evaluated the electric quadrupole shifts of a large number of transitions in HD^+, the hydrogen molecular ion most intensively studied with high-resolution optical spectroscopy to date. We have considered those radio-frequency, rotational, rovibrational one- and two-photon E1 transitions that have low, vanishing, or opposite equal Zeeman shifts and that are therefore of interest for precision spectroscopy. The radio-frequency (and rotational) transitions, for which the fractional uncertainty is higher than for the rovibrational ones, are of interest for a test of the hyperfine Hamiltonian of the molecule, while the the rovibrational transitions are of interest for QED tests, fundamental constants metrology and equivalence principle tests.

For the rovibrational transitions we find one-photon transitions of very low Zeeman shift and two-photon transitions that are free of Zeeman shift and of quadrupole shift. In the one-photon transitions of smallest quadrupole shift, it is of fractional magnitude close to 1×10^{-15}. However, if the nulling procedure is applied, the uncertainty in the residual quadrupole shift can be reduced to this level for essentially all rovibrational transitions.

Combining these considerations with earlier analyses of the blackbody shift and a recent precise evaluation of the Stark shift, we conclude that for a few selected rovibrational transitions of the HD^+ ion a fractional frequency uncertainty at the 5×10^{-16} level should be achievable, under realistic assumptions. This uncertainty is limited by the accuracy with which the systematic shifts can be determined, which is ultimately limited by the statistical uncertainty of measuring the transition frequencies. Because of the relatively short lifetimes of the vibrational levels, correspondingly long integration times are therefore necessary to reduce the statistical uncertainty to the above level.

We have not computed the shifts of individual energy levels of H_2^+ and D_2^+ in this paper. However, the numerical similarity of their coefficients E_{14} to those of HD^+ indicates that their quadrupole shifts will be similarly small. In this context, their distinctive feature is the extremely small natural linewidth of their transitions and the different spin structure of the transitions. Because of the smaller linewidth of the homonuclear ions, the statistical uncertainty can in principle be significantly lower than in HD^+. Thus, their potential for a molecular ion clock should be investigated in future studies.

Acknowledgments This work has been supported by Grant SCHI 431/19-1 of the Deutsche Forschungsgemeinschaft. We are grateful to V.I. Korobov and A. Bekbaev for making available to us their results of the polarizabilities and of the hyperfine Hamiltonian coefficients.

References

1. J.C.J. Koelemeij, B. Roth, A. Wicht, I. Ernsting, S. Schiller, Phys. Rev. Lett. **98**, 173002 (2007)
2. U. Bressel, A. Borodin, J. Shen, M. Hansen, I. Ernsting, S. Schiller, Phys. Rev. Lett. **108**, 183003 (2012)
3. V.I. Korobov, Z.-X. Zhong, Phys. Rev. A **86**, 044501 (2012)
4. J.-P. Karr, A. Douillet, L. Hilico, Appl. Phys. B **107**, 1043–1052 (2012). doi:10.1007/s00340-011-4757-z
5. A.K. Bekbaev, V.I. Korobov, M. Dineykhan, Phys. Rev. A **83**, 044501 (2011). doi:10.1103/PhysRevA.83.044501
6. U. Fröhlich, B. Roth, P. Antonini, C. Lämmerzahl, A. Wicht, S. Schiller, in *Seminar on Astrophysics, Clocks and Fundamental Constants*, eds. by E. Peik, S. Karshenboim. Lecture Notes in Physics, vol. 648 (Springer, Berlin, 2004), p. 297
7. S. Schiller, V.I. Korobov, Phys. Rev. A **71**, 032505 (2005)
8. M. Kajita, Phys. Rev. A **77**, 012511 (2008)
9. D. Bakalov, V.I. Korobov, S. Schiller, Phys. Rev. A **82**, 055401 (2010)
10. D. Bakalov, V.I. Korobov, S. Schiller, J. Phys. B At. Mol. Opt. Phys. **44**, 025003 (2011)
11. D. Bakalov, V.I. Korobov, S. Schiller, J. Phys. B At. Mol. Opt. Phys. **45**, 049501 (2012)
12. R.E. Moss, L. Valenzano, Mol. Phys. **100**, 1527 (2002)
13. J.-P. Karr, S. Kilic, L. Hilico, J. Phys. B At. Mol. Opt. Phys. **38**, 853 (2005)
14. J.C.J. Koelemeij, Phys. Chem. Chem. Phys. **13**, 18844 (2011)
15. D. Bakalov, S. Schiller, Hyperfine Interact. **210**, 25 (2012)
16. D.R. Bates, G. Poots, Proc. Phys. Soc. (Lond) Sec. A **66**, 784 (1953)
17. J.M. Peek, A. Hashemi-Attar, C.L. Beckel, J. Chem. Phys. **71**, 5382 (1979)
18. A.G. Posen, A. Dalgarno, J.M. Peek, At. Data Nucl. Data Tables **28**, 265–277 (1983)

19. H.O. Pilón, D. Baye, J. Phys. B: At. Mol. Opt. Phys. **45**, 065101 (2012). doi:10.1088/0953-4075/45/6/065101
20. D.M. Bishop, B. Lam, Chem. Phys. Lett. **134**, 283–287 (1987)
21. D.M. Bishop, B. Lam, Mol. Phys. **65**, 679–688 (1988)
22. A.K. Bhatia, R.J. Drachman, Phys. Rev. A **61**, 032503 (2000)
23. H.O. Pilón, Quadrupole transitions in the bound rotational–vibrational spectrum of the deuterium molecular ion. arXiv:1302.5234v2
24. D. Bakalov, V.I. Korobov, Phys. Rev. A **57**, 1662 (1998)
25. V.I. Korobov, D. Bakalov, Phys. Rev. Lett. **79**, 3379 (1997)
26. A.R. Edmonds, *Angular Momentum in Quantum, Mechanics*. (Princeton University Press, Princeton, 1957)
27. V.I. Korobov, D. Bakalov, H.J. Monkhorst, Phys. Rev. A **59**, R919 (1999)
28. D. Bakalov, V.I. Korobov, S. Schiller, Phys. Rev. Lett. **97**, 243001 (2006)
29. V.I. Korobov, Phys. Rev. A **77**, 022509 (2008)
30. H. Wind, J. Chem. Phys. **42**, 2371 (1965)
31. V.I. Korobov, Phys. Rev. A **74**, 052506 (2006)
32. H.J. Montgomery, Chem. Phys. Lett. **50**, 455–458 (1977). doi:10.1016/0009-2614(77)80365-5
33. N. Huntemann, M. Okhapkin, B. Lipphardt, S. Weyers, C. Tamm, E. Peik, Phys. Rev. Lett. **108**, 090801 (2012)
34. J. Shen, A. Borodin, M. Hansen, S. Schiller, Phys. Rev. A **85**, 032519 (2012)
35. W.M. Itano, J. Res. Natl. Inst. Stand. Technol. **105**, 829–837 (2000)
36. W.H. Oskay, S.A. Diddams, E.A. Donley, T.M. Fortier, T.P. Heavner, L. Hollberg, W.M. Itano, S.R. Jefferts, M.J. Delaney, K. Kim, F. Levi, T.E. Parker, J.C. Bergquist, Phys. Rev. Lett. **97**, 020801 (2006). doi:10.1103/Phys.Rev.Lett.97.020801.
37. V.I. Korobov, A. Bekbaev, S. Schiller, et al., in preparation.
38. D. Bakalov, K. Bakalova, V.I. Korobov, H.J. Monkhorst, I. Shimamura, Phys. Rev. A **57**, 3370 (1998)
39. P.E. Knowles, G.A. Beer, G.R. Mason et al., Phys. Rev. A **56**, 1970 (1998)